

RESEARCH ARTICLE

Ethanol Disrupts Hormone-Induced Calcium Signaling in Liver

Lawrence D. Gaspers ^{1,*}, Andrew P. Thomas¹, Jan B. Hoek², Paula J. Bartlett¹

¹Department of Pharmacology, Physiology and Neuroscience, New Jersey Medical School, Rutgers, The State University of New Jersey, Newark, NJ 07103, USA; ²Department of Pathology, Anatomy and Cell Biology, Thomas Jefferson University, Philadelphia, PA 19107, USA

*Address correspondence to L.D.G. (e-mail: larry.gaspers@rutgers.edu)

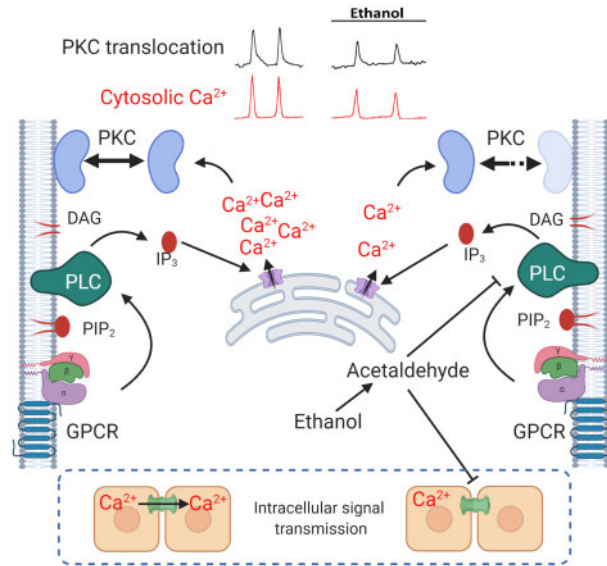
Abstract

Receptor-coupled phospholipase C (PLC) is an important target for the actions of ethanol. In the ex vivo perfused rat liver, concentrations of ethanol >100 mM were required to induce a rise in cytosolic calcium (Ca²⁺) suggesting that these responses may only occur after binge ethanol consumption. Conversely, pharmacologically achievable concentrations of ethanol (≤30 mM) decreased the frequency and magnitude of hormone-stimulated cytosolic and nuclear Ca²⁺ oscillations and the parallel translocation of protein kinase C-β to the membrane. Ethanol also inhibited gap junction communication resulting in the loss of coordinated and spatially organized intercellular Ca²⁺ waves in hepatic lobules. Increasing the hormone concentration overcame the effects of ethanol on the frequency of Ca²⁺ oscillations and amplitude of the individual Ca²⁺ transients; however, the Ca²⁺ responses in the intact liver remained disorganized at the intercellular level, suggesting that gap junctions were still inhibited. Pretreating hepatocytes with an alcohol dehydrogenase inhibitor suppressed the effects of ethanol on hormone-induced Ca²⁺ increases, whereas inhibiting aldehyde dehydrogenase potentiated the inhibitory actions of ethanol, suggesting that acetaldehyde is the underlying mediator. Acute ethanol intoxication inhibited the rate of rise and the magnitude of hormone-stimulated production of inositol 1,4,5-trisphosphate (IP₃), but had no effect on the size of Ca²⁺ spikes induced by photolysis of caged IP₃. These findings suggest that ethanol inhibits PLC activity, but does not affect IP₃ receptor function. We propose that by suppressing hormone-stimulated PLC activity, ethanol interferes with the dynamic modulation of [IP₃] that is required to generate large, amplitude Ca²⁺ oscillations.

Submitted: 18 November 2020; Revised: 22 December 2020; Accepted: 30 December 2020

© The Author(s) 2021. Published by Oxford University Press on behalf of American Physiological Society.

This is an Open Access article distributed under the terms of the Creative Commons Attribution Non-Commercial License (<http://creativecommons.org/licenses/by-nc/4.0/>), which permits non-commercial re-use, distribution, and reproduction in any medium, provided the original work is properly cited. For commercial re-use, please contact journals.permissions@oup.com



Key words: ethanol; inositol 1,4,5-trisphosphate; gap junctions; receptor-coupled phospholipase c; calcium signaling

Introduction

Calcium mobilization from intracellular stores and Ca^{2+} -influx from the extracellular space are ubiquitous signals used to control a wide range of cellular processes.¹⁻⁵ Calcium-mobilizing hormones, such as α_1 -adrenergic receptor agonists and vasopressin, regulate liver function by activating the phosphoinositide-specific phospholipase C (PI-PLC) signaling cascade to produce transient increases in cytosolic free calcium concentration ($[\text{Ca}^{2+}]_i$). Increases in $[\text{Ca}^{2+}]_i$ are achieved by the activation of receptor-associated trimeric G proteins (G_q/G_{11}), stimulation of PLC β activity, hydrolysis of the lipid precursor phosphatidylinositol 4,5-bisphosphate, and the corelease of the second messenger's inositol 1,4,5-trisphosphate (IP_3) and diacylglycerol (DAG). DAG stimulates the activity of protein kinase C (PKC), while IP_3 binds to receptors in the endoplasmic reticulum to release internal Ca^{2+} stores.^{1,6} Depletion of the internal Ca^{2+} stores, in turn, stimulates store-operated calcium entry to sustain the hormone signal and refill the internal Ca^{2+} stores.⁷ In nonexcitable cells, such as pancreatic acinar cells and hepatocytes, these Ca^{2+} signals are manifest as periodic Ca^{2+} increases referred to as Ca^{2+} oscillations, and the individual Ca^{2+} transients propagate across the cell from a discrete origin as Ca^{2+} waves. The frequency of Ca^{2+} oscillations is determined by the concentration of the hormone, while the amplitude and kinetics of individual $[\text{Ca}^{2+}]_i$ spikes as well as the rates at which the Ca^{2+} increase propagates across the cell are largely independent of agonist dose.⁸⁻¹⁰ These oscillatory calcium signals are rapidly transferred into the mitochondrial matrix thereby stimulating Ca^{2+} -sensitive dehydrogenases leading to enhanced production of NAD(P)H^{11,12} and synthesis of mitochondrial ATP.⁵ PLC-linked $[\text{Ca}^{2+}]_i$ spikes also propagate into the hepatocyte nucleus¹³ stimulating the activity of Ca^{2+} -sensitive transcription factors and kinases that, in turn, regulate cell proliferation and responses to acute liver injury.^{14,15}

Previous studies have identified multiple sites of interaction between ethanol intoxication and the phosphoinositide signaling system. In pancreatic acinar cells, nonoxidative metabolites of ethanol can mobilize internal Ca^{2+} stores through an IP_3 receptor mechanism, whereas ethanol targets the activity of PLC in hepatocytes.^{16,17} The addition of ethanol to isolated hepatocyte suspensions, in the absence of receptor agonists, has been shown to stimulate receptor-coupled PLC, evident by the accumulation of [^3H]inositol, a rise in $[\text{Ca}^{2+}]_i$, and the Ca^{2+} -dependent activation of phosphorylase a.¹⁸ However, ethanol-stimulated PLC activity requires high concentrations of ethanol (≥ 100 mM), is short-lived and followed by desensitization of the pathway. The direct ethanol-induced Ca^{2+} increases are also sensitive to experimental conditions, and are either absent or markedly diminished in hepatocytes maintained in primary culture.¹⁹⁻²¹ Importantly, it is unclear if blood alcohol concentrations can rise to the levels that activate PLC in vivo except after excessive binge ethanol intake,²²⁻²⁴ or if these Ca^{2+} signals play a role in the development of liver injury.

It has also been documented that acute ethanol treatment suppresses the cellular responses to multiple hormones coupled to the activation of PLC β .^{17,21,25,26} Here, the ethanol concentrations required to inhibit receptor-coupled PLC activity are lower compared to those required to activate the enzyme directly and are unaffected by culture conditions. Moreover, the mechanism by which ethanol suppresses PLC is thought to be distinct from the actions of ethanol that result in the activation of PLC.²⁷ The sites of acute ethanol action have not been fully defined. Ethanol may interfere with receptor-G protein coupling and/or potentiate a PKC-dependent negative feedback loop onto PLC activity.^{17,21,25,26} Either mechanism could explain the decrease in hormone-stimulated production of IP_3 . Ethanol has also been reported to inhibit IP_3 binding and to reduce the

efficacy of IP₃ to activate the intracellular IP₃-gated Ca²⁺ release channels in digitonin-permeabilized hepatocytes.²⁸ Perturbing IP₃ receptor function would also contribute to the suppression of PLC-linked Ca²⁺ signals.

We have previously shown that hepatocytes are desensitized to the inhibitory actions of acute ethanol treatment on hormone-induced Ca²⁺ signals after chronic ethanol feeding. Hepatocytes isolated from ethanol-fed rats or mice exhibit higher levels of receptor-mediated PLC activity and a leftward shift in the dose-response curves for Ca²⁺-mobilizing stimuli, resulting in more sustained increases in [Ca²⁺]_i at low hormone concentrations rather than the typical oscillatory Ca²⁺ signals.²⁹ These compensatory mechanisms would allow the liver to respond to Ca²⁺-mobilizing hormones even in the presence of intoxicating levels of ethanol, but may also predispose the tissue to further ethanol-induced injury by causing Ca²⁺ overload or over stimulation of PKC during periods of ethanol withdrawal.

There is increasing evidence that dysregulation in Ca²⁺ handling and Ca²⁺ signaling is a potential driver in the development of numerous liver diseases including nutrient-induced fatty liver disease,^{30–35} hepatic insulin resistance,^{36,37} cholestasis,^{38,39} liver regeneration,^{14,40} hepatocellular carcinoma,⁴¹ and metastases.^{4,42–46} In this study, we first demonstrate that ethanol concentrations >100 mM are required to induce [Ca²⁺]_i increases in hepatocytes within the intact perfused rat liver. These ethanol-induced Ca²⁺ oscillations occurred in small numbers of cells and may only manifest after a high dose of acute ethanol feeding. By contrast, ethanol concentrations that are readily achievable in vivo potentially inhibit hormone-induced Ca²⁺ oscillations and decrease the magnitude of both cytosolic and nuclear Ca²⁺ oscillations in the ex vivo perfused liver. Moreover, these levels of ethanol also inhibited gap junction communication in intact liver, causing the loss of coordinated and spatially organized intercellular Ca²⁺ waves, which are thought to synchronize the metabolic output of the liver.⁴⁷ The actions of ethanol on hormone-stimulated Ca²⁺ oscillations required metabolism and were largely prevented by pretreatment with 4-methylpyrazole, an alcohol dehydrogenase inhibitor, indicating a role for acetaldehyde in inhibiting IP₃/PLC-linked Ca²⁺ oscillations. Ethanol treatment decreased both the rate of rise and magnitude of hormone-stimulated IP₃ formation. We predict that by slowing down the dynamic changes in [IP₃], ethanol interferes with Ca²⁺-IP₃ cross-coupling causing the early termination of [Ca²⁺]_i spikes. Indeed, increasing the concentration of the hormone and presumably enhancing the rates of IP₃ production overcame the effects of ethanol on the frequency of Ca²⁺ oscillations and amplitude of the Ca²⁺ spike. Ethanol-dependent inhibition of receptor-operated Ca²⁺ oscillations was paralleled by the loss of conventional PKCβ translocation to the membrane. Taken together, this study demonstrates that acute ethanol intoxication suppresses receptor-mediated activation of PLC, which translates into the bilateral inhibition of both Ca²⁺ and PKC signaling pathways in hepatocytes.

Materials and Methods

Reagents

Hydroxyethyl piperazineethanesulfonic acid (HEPES) and all other chemicals were obtained from Sigma-Aldrich (St Louis, MO, USA) or VWR BDH chemicals (Radnor, PA, USA). Fura-2/AM, fluo-4/AM, calcein/AM, pluronic acid F-127, and fluorescein conjugated-BSA were obtained from Thermo Fisher Scientific

(Waltham, MA, USA), bromosulphophthalein (BSP) was from Fluka (Fluka, Buchs, Switzerland), and 190 proof ethyl alcohol from Decon, Labs Inc. Heat shock, fraction V BSA was from Roche (Basel, Switzerland). BSA was extensively dialyzed against normal saline plus 10 mM HEPES using Spectra/Por 12–14 kDa cut-off dialysis tubing (Thermo Fisher Scientific).

Dr. K. Mikoshiba (RIKEN) generously provided the plasmid pIRIS-1 and pRatiometric-pericam-nu was a gift from A. Miyawaki (RIKEN). pGP-CMV-GCaMP6f was a gift from Douglas Kim & GENIE Project (Addgene plasmid # 40755; <http://n2t.net/addgene:40755>; RRID:Addgene_40755). Adenovirus particles expressing PKCβII-enhanced green fluorescent protein (Ad-PKCβII-EGFP) were a gift from Dr. R. Rizzuto (University of Padua).

Ethical Approval and Animals

Animal studies were approved by the Institutional Animal Care and Use Committee at Rutgers, New Jersey Medical School. Male Sprague Dawley rats (weighing 200–250 g; Taconic Biosciences, Rensselaer, NY, USA) were housed in ventilated cages under a 12:12 h dark:light cycle in a fully Association for Assessment and Accreditation of Laboratory Animal Care (AAALAC) accredited animal facility. Rats were given ad libitum access to rodent chow and water until the day of experimentation. Rats were anesthetized with an I.P. injection of Nembutal (60 mg/kg, Diamondback Drugs, Scottsdale, AZ, USA) diluted 1:1 with PBS. The depth of anesthesia was assessed by relaxation of muscle tone and a loss of reflex responses to external stimuli. Liver tissue was harvested under a surgical plane of anesthesia and used for isolation of hepatocytes or establishing ex vivo perfused liver preparations. The organ donor did not recover from surgery.

Adenovirus Production

Ad-PKCβII-EGFP virus particles were produced in HEK 293 cells. EGFP expression was used to monitor production of viruses. Virus particles were extracted, purified by ultracentrifugation on a CsCl gradient then dialyzed extensively against 20 mM Tris, pH 8.0, 25 mM NaCl, and 2.5% glycerol. Viral stocks (10¹³ particles/mL) were stored at –80 °C until used.

Ex vivo Perfused Liver

The livers of anesthetized male Sprague Dawley rats (200–250 g) were perfused in situ via the hepatic portal vein with a HEPES-buffered balanced salt solution (HBSS) as described previously.^{48–50} The perfusion buffer was composed of (in mM): 121 NaCl, 25 Hepes (pH 7.4 at @30°C), 5 NaHCO₃, 4.7 KCl, 1.2 KH₂PO₄, 1.2 MgSO₄, 1.3 CaCl₂, 5.5 glucose, 0.5 glutamine, 3 lactate, 0.3 pyruvate, 0.2 BSP, and 0.1% (w/v) dialyzed BSA, equilibrated with 100% O₂ at 30°C. BSP, an organic anion transport inhibitor, was included to inhibit efflux of Ca²⁺ indicator dyes.^{48–50} The median lobe of the liver was used for these studies and other lobes were tied off with silk thread and excised to increase the loading efficiency of indicator dyes for confocal imaging. Ca²⁺-sensitive indicator dyes or calcein/AM were loaded by recirculating perfusion buffer supplemented with 5 μM of the acetoxymethyl ester, 0.02% (v/v) Pluronic F-127, and 2% (w/v) dialyzed BSA for 40–50 min. Following dye loading, the liver was transferred to a custom-built imaging chamber fitted onto the microscope stage as described previously.^{48–50}

Hepatocyte Isolation and Culture

Hepatocytes were isolated by a two-step collagenase perfusion of livers from fed male Sprague Dawley rats essentially as described previously.¹² Hepatocytes (500 000–750 000 cells) were plated onto glass coverslips coated with type 1 collagen (rat tail, Corning; 10 $\mu\text{g}/\text{cm}^2$). Cells were maintained for 30–60 min in a humidified atmosphere of 5% CO_2 and 95% air at 37°C in complete Williams' Medium E (WEM, Thermo Fisher Scientific) supplemented with 5% (v/v) fetal bovine serum (Atlanta Biologicals), penicillin, (10 units/mL), streptomycin (10 $\mu\text{g}/\text{mL}$), gentamycin sulfate (50 $\mu\text{g}/\text{mL}$), and glutamine (2 mM). In some experiments, hepatocytes were transduced with Ad-PKC β II-EGFP (100 particles/cell) or transfected by electroporation using an Amaxa Rat/Mouse Hepatocyte Nucleofector Kit according to the manufacturer's instructions (Lonza, Basel, Switzerland). Hepatocytes used in electroporation or viral transduction protocols were maintained in complete WEM containing 140 nM insulin for 3–4 h and then insulin was reduced to 14 nM and the cells cultured for an additional 16–20 h to allow expression of the transgene.

Imaging Measurements of $[\text{Ca}^{2+}]_i$ in the ex vivo Perfused Liver

Confocal images were acquired with a Radiance 2002-MP laser scanning multiphoton confocal microscope (Bio-Rad, Hercules, CA, USA) using either 10 \times 0.5 NA or 20 \times 0.75 NA PlanFluor objectives (Nikon, Tokyo, Japan) using the manufacturer's software as described previously.⁴⁷ A Mira/Verdi Ti:sapphire laser (Coherent Inc. Santa Clara, CA, USA) was used for multiphoton excitation of the fura-2 and the 488 nm argon laser line was utilized for single-photon excitation of fluo-4. Fura2 images (810 nm excitation, 460–600 nm emission) and fluo-4 images (488 nm excitation, 520–600 nm emission) were captured every 4 s. At the end of the experiment, fluorescein-labeled BSA (F-BSA) was injected into the perfusion line to identify the different lobular zones as described previously.^{48–50} In some experiments, fura-2 fluorescence (excitation 340 and 380 nm, emission 420–600 nm) was also detected using a cooled charge-coupled device (CCD) camera (Photometrics) as described previously.^{48–50} Values for $[\text{Ca}^{2+}]_i$ were calculated from the 340/380 nm ratio after correction for autofluorescence and out of focus information as described in^{48–50} Autofluorescence images were acquired by perfusing the liver for 10–15 min with 100 μM MnCl_2 in Ca^{2+} -free HBSS buffer to quench cytosolic fura-2, and images were deblurred with deconvolution algorithms to remove out of focus fluorescence.⁵¹

When applicable, minor movements of the liver tissue in the x,y direction were corrected using the StackReg plugin for ImageJ.⁵² Hormone-induced increase in fura-2 or fluo-4 fluorescence intensities were analyzed using in-house software or algorithms written for ImageJ (NIH, Bethesda, MD, USA). The lobular organization of hormone-induced increases in Ca^{2+} is shown as the actual fluorescence intensity values depicted on a linear gray scale with the magnitude of increases in $[\text{Ca}^{2+}]_i$ at each time point shown with a red overlay as described previously.^{10,48} Changes in $[\text{Ca}^{2+}]_i$ were calculated by subtracting sequential confocal images to yield a differential image stack and the fluorescence intensity at each time point is proportional to the change in Ca^{2+} . Difference images were processed with a median filter and a minimum threshold intensity to reduce noise.

Fluorescence Recovery after Photobleaching

Fluorescence recovery after photobleaching (FRAP) experiments were carried out in calcein/AM-loaded livers. Routines written in the manufacturer's macro language were used to control the bleaching laser pulse and image acquisition. Photobleaching was carried out by briefly focusing the laser onto a single hepatocyte and then acquiring full-field images. Confocal images of calcein fluorescence were acquired every 5–10 s using a Bio-Rad MRC-600 laser scanning confocal microscope (488 nm excitation, 515–600 nm emission) and a 60 \times 1.3 NA SPlan objective. A linear fit was used to calculate the initial rate of fluorescence recovery.

Single-Cell Imaging Measurements and Data Analysis

Single-cell imaging experiments were performed in HBSS containing 100–200 μM sulfobromophthalein and 0.25% (w/v) BSA, pH 7.4 at 37°C. Cell cultures were loaded with fura-2 by incubation with 2–5 μM fura-2/AM plus Pluronic F-127 (0.02% v/v) for 20–40 min in HBSS. The cells were washed twice with HBSS and then transferred to a thermostatically regulated microscope chamber (37°C). Fura-2 fluorescence images (excitation, 340 \pm 10 and 380 \pm 10 nm, emission 420–600 nm) were acquired at 3–4 s intervals with a cooled CCD camera as previously described.^{53,54} Calibration of fura-2 in terms of $[\text{Ca}^{2+}]_i$ was calculated from the 340/380 nm ratio after correcting for cellular autofluorescence.⁵⁵ Autofluorescence values were obtained at the end of each experiment by permeabilizing the cells with digitonin in an intracellular-like media containing a Ca^{2+} /EGTA buffer and Mg-ATP to release cytosolic fura-2. The fura-2 calibration parameters were determined in vitro using a Kd value of 224 nM. For simultaneous measurement of hormone-induced $[\text{Ca}^{2+}]_i$ and PKC β II-EGFP responses, fura-2-loaded hepatocytes were excited with 340, 380, and 485 nm, using a computer-controlled filter wheel and shutter. The emitted fluorescence was collected using a fura-2/BCECF dichroic beam splitter and a 515 nm long bandpass emission filter (Chroma Technology) as described previously.⁵³ For these experiments, the fura-2 ratio was not converted into $[\text{Ca}^{2+}]_i$ due to a small amount of EGFP contamination into the fura-2 fluorescence intensity signal. Changes in PKC β II-EGFP distribution were monitored by taking the ratio of the GFP fluorescence intensity changes in the membrane versus cytosol. The resulting membrane:cytosol ratio was normalized to the baseline values prior to data analysis. The amplitude, rate of rise, rate of decline, and area under the curve (AUC) for $[\text{Ca}^{2+}]_i$ spikes and the translocation of PKC β II-EGFP to the membrane were determined using algorithms (Brumer R & Thomas A, unpublished work) written in MATLAB (MathWorks, Natick, MA, USA).

Flash Photolysis of Caged IP_3

Cytosolic calcium changes induced by photolysis of caged IP_3 were measured using the Ca^{2+} indicator fluo4-AM. Cells were loaded with 2 μM caged IP_3 (Sichem GmbH) in HBSS for 45 min; followed by 30 min with 5 μM fluo4/AM. Cells were washed and mounted on the stage of an Axiovert200 (Zeiss) spinning disc confocal microscope. Fluo4 fluorescence images (Argon laser excitation 488 nm, emission >510 nm) were acquired at 2 Hz with a CCD camera using the data acquisition software Piper Control™ (Stanford photonics). Photolysis of caged IP_3 was achieved by light pulses (1 ns duration with a wavelength of 337 nm and 1.45 mJ of energy) from a nitrogen-charged UV flash lamp (Photon Technology International) guided through the

objective (C-Achromatx20/1.2). Data analysis was performed using ImageJ (NIH).

Simultaneous Measurement of $[Ca^{2+}]_i$ and IRIS-1 in Single Cells

Hepatocytes were transfected with 2–5 μ g of IRIS-1 via electroporation (NucleofectorTM; Lonza), plated onto collagen (10 μ g/cm³)-coated glass coverslips then cultured overnight in insulin-containing WEM. Transfected cultures were incubated with 1 μ M indo-1/AM and Pluronic acid F-127 (0.02% v/v) for 20–30 min at 37°C in HBSS. Simultaneous indo-1 and IRIS-1 fluorescence images were acquired by sequential illumination with 436 \pm 20 nm then 360 \pm 40 nm excitation using a 455 nm long bandpass dichroic mirror. IRIS-1 donor and acceptor fluorescence images were separated with a 505 nm long bandpass dichroic mirror and directed to 480 \pm 30 nm (CFP) or 535 \pm 40 nm (Venus) emission filters using an image beam splitter (Optical InsightsTM). The CFP donor emission image recorded at 480 nm was divided by the acceptor emission image recorded at 535 nm to obtain the FRET emission ratio.⁵⁶ Indo-1 fluorescence intensities decrease with increasing $[Ca^{2+}]_i$ in both emission channels. These images are summed to increase the signal output and reported as the ratio of $(F/F_0)^{-1}$.

Statistical Analysis

Data are presented as means \pm SD for the number of livers, separate hepatocyte preparations, or cells as indicated in the figure legend. Statistical differences from the relevant controls were calculated by Student's *t*-test or one-way ANOVA for more than two groups (Prism; GraphPad Software Inc., San Diego, CA, USA). A value of $P < 0.05$ was considered statistically significant.

Results

High Doses of Ethanol Induce $[Ca^{2+}]_i$ Spikes in the ex vivo Perfused Liver

Relatively high concentrations of ethanol have previously been shown to induce $[Ca^{2+}]_i$ increases in hepatocyte suspensions by activating receptor-coupled PLC activity.^{18,25,57,58} In this study, we tested whether lower concentrations of ethanol can also induce $[Ca^{2+}]_i$ spikes in the ex vivo perfused liver; a tissue preparation that maintains the normal architecture of the liver and cell-to-cell communication. Perfused rat livers were loaded with Ca^{2+} -sensitive indicator dyes (see “Materials and Methods” section) and challenged with increasing concentrations of ethanol. Live tissue confocal imaging studies revealed that concentrations of ethanol up to 30 mM did not induce Ca^{2+} responses after 10–20 min of perfusion (not shown), whereas ethanol concentrations ≥ 100 mM induced $[Ca^{2+}]_i$ oscillations in a few hepatocytes scattered throughout the liver lobule. Increases in $[Ca^{2+}]_i$ were detected in about 1% of the cells within a field of view after perfusion with 100 mM ethanol ($1.2 \pm 1.3\%$; mean \pm SD, $n = 3$ livers) and increased to about 5–10% in the presence of 300 mM (Figure 1A; $6 \pm 8\%$; mean \pm SD, $n = 3$). In Figure 1A, the red overlay was created from a maximal projection throughout time of a differential image series, showing the peak $[Ca^{2+}]_i$ increase in all the responsive hepatocytes during the 10 min perfusion period. The red color shows the lobular distribution of ethanol-responsive cells, confined predominately to the periportal regions, and the color intensity reflects the magnitude of ethanol-induced Ca^{2+} activity. The traces in Figure 1B show the $[Ca^{2+}]_i$ responses in two adjacent cells along the same hepatic

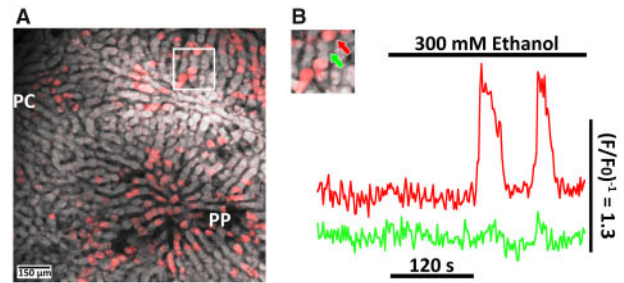


Figure 1. High Doses of Ethanol Stimulate Asynchronous $[Ca^{2+}]_i$ Increases in the Perfused Liver. A rat liver loaded with fura-2/AM was perfused with 300 mM ethanol for 10 min. (A) A differential image time series was calculated to localize positive $[Ca^{2+}]_i$ changes, and this was used to generate a maximum intensity projection (red) superimposed on the original fluorescence image (gray). Thus, the red overlay shows the location of ethanol responsive cells and the color intensity reflects the peak Ca^{2+} . The white box shows the area displayed as an insert in panel b at higher resolution. (B) Colored traces are the $[Ca^{2+}]_i$ responses in two adjacent hepatocytes during the perfusion with ethanol (bar). The lobular location of the cells is depicted by the similarly colored arrows shown on the insert.

plate after perfusing the liver with 300 mM ethanol. The data indicate that ethanol-induced $[Ca^{2+}]_i$ increases are asynchronous and do not propagate as intercellular Ca^{2+} waves, as shown for Ca^{2+} -mobilizing hormones, eg, see Figure 2A. The biological significance of these high ethanol-induced Ca^{2+} responses is not clear as these levels are not typically achieved in animal models of ethanol feeding⁵⁹ and may only occur in extremely intoxicated individuals (see “Discussion” section). Therefore, we decided to focus on ethanol actions on hormone-induced Ca^{2+} signaling, as these effects occur at lower pharmacologically relevant ethanol concentrations.

Acute Ethanol Treatment Inhibits Hormone-Induced Intercellular Ca^{2+} Waves in the Intact Liver

As reported previously,^{48,60} perfusion with submaximal concentrations of vasopressin (30–100 pM) initially induce periodic $[Ca^{2+}]_i$ spikes (oscillations) in a small number of hepatocytes surrounding the periportal tract, which then spread progressively along the hepatic plates generating a wave of $[Ca^{2+}]_i$ increase throughout the liver lobule (Figure 2A). The average frequency of vasopressin-induced Ca^{2+} oscillations was 0.71 ± 0.2 and 0.66 ± 0.2 spikes/min (mean \pm SD, $n = 17$ livers) in the periportal and pericentral zones, respectively. In the continuous presence of hormone, each Ca^{2+} spike generated in the initiating periportal cells propagated throughout the lobule as an intercellular Ca^{2+} wave. The images in Figure 2B show the effect of perfusing the same liver with 20 mM ethanol in the continuing presence of the vasopressin. The arrival of ethanol into the lobule often induced a $[Ca^{2+}]_i$ increase in a few cells scattered throughout field of view (Figure 2B, 15 s), and this was followed by a strong inhibition of vasopressin-induced Ca^{2+} oscillations and the loss of coordinated intercellular Ca^{2+} waves (Figure 2B, 45–105 s). Experiments carried out at higher magnification revealed that Ca^{2+} spikes generated within pacemaker-like hepatocytes⁴⁸ did not propagate from cell-to-cell along the hepatic plate in the presence of ethanol, suggesting that gap junction communication was impaired (Figure 2C).

The frequency of the Ca^{2+} oscillations elicited by vasopressin in the intact liver was calculated in the absence and presence of ethanol in the perfusate, and the data expressed as a

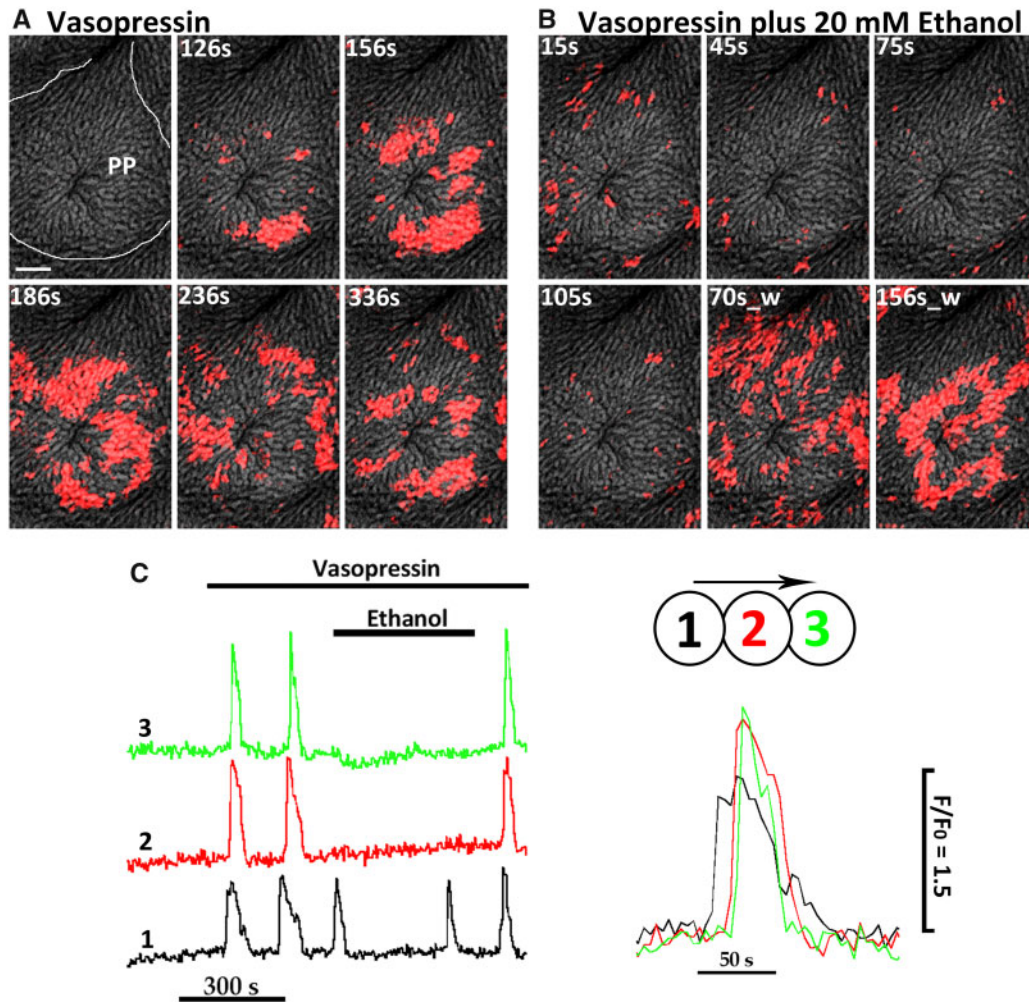


Figure 2. Effect of Acute Ethanol Treatment on Vasopressin-Induced Intercellular Ca^{2+} Waves in the Intact Liver. (A and B) A fluo-3/AM loaded rat liver was infused with 100 pM vasopressin (A) followed by perfusion with 20 mM ethanol in the continuing presence of vasopressin (B). Confocal images ($563 \mu\text{m} \times 686 \mu\text{m}$) of fluo-3 fluorescence are displayed in a linear grayscale with increases in fluorescence intensity at each time point displayed as a red overlay. Time (s) after vasopressin (A, 126–336 s) or ethanol (B, 15–105 s) reach the liver are shown in the top left of each image. In (B), the bottom right two panels show the Ca^{2+} response at 70 s and 156 s (70 s_w, 156 s_w) after beginning the washout of ethanol. Periportal (PP) zone and the boundary (white line) of a lobule are illustrated in the first image of Panel A. White scale bar denotes 100 μm . (C) Traces are the $[\text{Ca}^{2+}]_i$ responses from three hepatocytes positioned sequentially along a hepatic plate. The Ca^{2+} traces are displaced along the y-axis for clarity. The insert on the right shows the cell-to-cell propagation of one Ca^{2+} spike induced by vasopressin. The colors and numbers of the cells correspond to the similar colored and numbered Ca^{2+} traces. Data were acquired at higher magnification ($\times 20$) in a separate liver preparation.

fold-change. Ethanol reduced the frequency of hormone-induced Ca^{2+} oscillations in a dose-dependent fashion in hepatocytes located in both the periportal and pericentral zones, with IC_{50} values of 1.4 and 2 mM, respectively (Figure 3A and B). In addition to its effects on the rates of Ca^{2+} spiking, ethanol also decreased the magnitude of vasopressin-induced $[\text{Ca}^{2+}]_i$ increases. This effect is best seen in fura-2/AM loaded livers where the ratiometric method can be used to control for tissue movement and dye leakage (Figure 3C). The effect of ethanol on the amplitude of $[\text{Ca}^{2+}]_i$ spikes was also observed in isolated hepatocytes (see below). The action of ethanol on hormone-induced Ca^{2+} oscillations was fully reversible (Figure 2C), and spatially organized intralobular Ca^{2+} waves reformed 1–2 min after commencing the washout of ethanol (Figure 2B, 70 s_w, 156 s_w). Increasing the concentration of vasopressin in the perfusate also overcame the inhibitory effects of ethanol on the frequency of Ca^{2+} oscillations (Figure 3D and E). However, even with increased vasopressin, the Ca^{2+} responses in the presence

of ethanol were still not organized on a lobular scale, and intercellular Ca^{2+} waves propagated through only a small number of cells before terminating. These findings suggest that actions of ethanol on the Ca^{2+} oscillation machinery can be overcome by increasing the rate of IP_3 formation, but the higher levels of IP_3 are not capable of reversing the effects of ethanol on gap junction communication.

Ethanol Inhibits Gap Junction Communication in the ex vivo Perfused Liver

Gap junctions are one target for the inhibitory actions of ethanol⁶¹ and loss of intercellular communication could help to explain the disruption of intercellular Ca^{2+} waves (Figure 2B). Previous studies have demonstrated the ability to assess gap junction communication by monitoring the rates of FRAP in both isolated hepatocyte couplets⁶² and hepatocytes within the perfused liver.⁶³ Here, ex vivo perfused rat livers were loaded

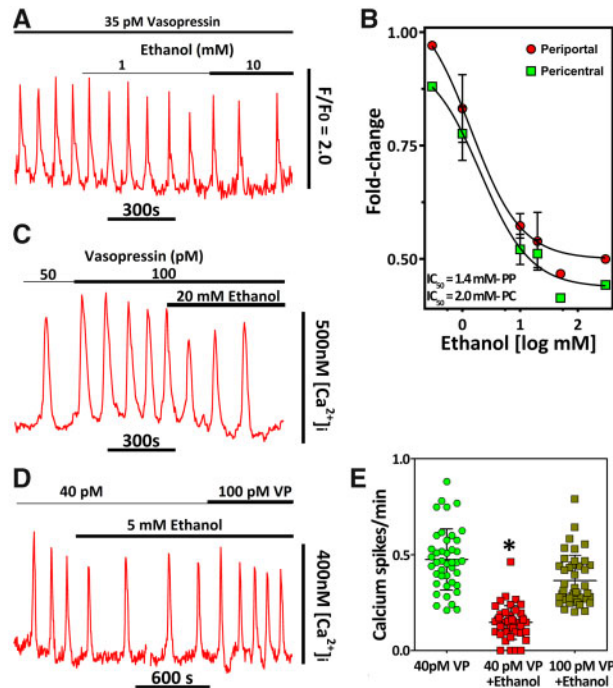


Figure 3. Effect of Acute Ethanol Administration on Vasopressin-Induced Ca^{2+} Signaling in the Perfused Liver. (A) Single-cell $[\text{Ca}^{2+}]_i$ trace showing the effects of increasing concentrations of ethanol on vasopressin-induced Ca^{2+} oscillations in the intact perfused liver. The concentrations and duration of vasopressin and ethanol perfusion are shown by the horizontal bars. (B) The frequency of $[\text{Ca}^{2+}]_i$ spiking induced by vasopressin (30–100 pM) was determined in single hepatocytes within the periportal (PP, red) or pericentral (PC, green) zones (30–125 cells/zone/liver) in the absence and presence of ethanol in the perfusion buffer. The data are expressed as the fold-change for the indicated ethanol concentrations. Data were acquired from fura-2/AM or fluo-4/AM loaded livers ($n=17$ livers). Symbols are the mean \pm SD, or mean data for experiments with less than three livers (see also Table 1). (C–E) Fura-2/AM-loaded rat livers were stimulated with vasopressin (VP) followed by perfusion with ethanol plus hormone at the indicated concentrations. Fura-2 fluorescence images were deconvolved prior to calculating the ratio as described previously.⁴⁸ (E) Summary data from the experiment shown in Panel D, depicting the frequency as Ca^{2+} spikes per minute for the indicated conditions. Rates of Ca^{2+} spiking were determined in individual hepatocytes from two different lobules. *Significantly different from other conditions; one-way ANOVA, Tukey post hoc test $P < 0.01$.

with a Ca^{2+} -insensitive indicator dye, calcein/AM, followed by a brief laser-induced photobleaching of a single hepatocyte or cluster of hepatocytes and fluorescence recovery monitored by confocal microscopy (Figure 4A). The FRAP assay was carried out before and then after perfusing the liver for 5–10 min with 20 mM ethanol in the same hepatic lobule, but using different hepatocytes for each assay to avoid laser-induced injury (Figure 4B). The initial rates of fluorescent recovery were determined, and summary data are presented in Figure 4C. The data indicate that ethanol perfusion markedly inhibits the rate of fluorescence recovery. These results are consistent with acute ethanol intoxication suppressing gap junction communication, which could explain the loss of coordinated propagating intercellular Ca^{2+} waves.

The Effects of Ethanol on Hormone-Induced Ca^{2+} Oscillations in Isolated Hepatocytes

The remaining experiments in this study were carried out in primary cultured hepatocytes, which maintain the hormone-

stimulated Ca^{2+} oscillation properties described above for the intact liver.^{8–10} Consistent with the intact liver data, the addition of ethanol inhibited Ca^{2+} oscillations induced by either phenylephrine, an α_1 -adrenergic agonist, or vasopressin in fura-2/AM loaded hepatocytes (Figure 5A and B). In some experiments, hepatocytes were transfected with genetically encoded calcium indicators (GECIs) targeted to the cytosol or nucleus, and then maintained in primary culture overnight. We used GECIs for these experiments because these biosensors can be selectively targeted within the cell, and they are also relatively immobile Ca^{2+} binding proteins, thus less likely to perturb local calcium dynamics. The traces in Figure 5C and D show examples of vasopressin-induced Ca^{2+} oscillations measured with GCaMP6f fluorescence before and after addition of 30 mM ethanol. Ethanol addition caused a modest but persistent decrease in the peak height of GCaMP6f Ca^{2+} oscillations (Figure 5C) or a progressive loss in peak height until Ca^{2+} spiking ceased (Figure 5D). The amplitude of hormone-induced GCaMP6f spikes decreased an average of $13 \pm 8\%$ after the addition of ethanol (mean \pm SD, $n=10$ GCaMP6f expressing hepatocytes from two cell preparations and four independent transfections, $P < 0.01$ paired t-test). Addition of a higher concentration of vasopressin reversed the effects of ethanol on both magnitude and frequency of cytosolic Ca^{2+} oscillations measured with GCaMP6f (Figure 5D). When added in the absence of hormone, ethanol (1–50 mM) had no effect on $[\text{Ca}^{2+}]_i$ (not shown).

We have previously demonstrated that intracellular Ca^{2+} waves propagate into the hepatic nucleus initiating a rise in nucleoplasmic $[\text{Ca}^{2+}]_i$.¹³ Hepatocyte cultures were transfected with ratiometric-pericam-nu to investigate the effects of ethanol treatment on nuclear Ca^{2+} signals. Notably, the acute addition of ethanol decreased both the frequency and amplitude of vasopressin (Figure 5E) or phenylephrine (Figure 5F) stimulated Ca^{2+} oscillations in the nucleoplasm. The magnitude of vasopressin-induced nuclear Ca^{2+} spikes decreased an average of $11 \pm 7\%$ after the addition of 30 mM ethanol (mean \pm SD, $n=6$ hepatocytes from three different cell preparations, $P < 0.05$ paired t-test). Similarly, the nuclear Ca^{2+} spikes generated by α_1 -adrenergic stimulation were also suppressed by ethanol treatment, with a decrease in amplitude of $10 \pm 4\%$ (mean \pm SD, $n=6$ hepatocytes from two different cell preparations, $P < 0.01$ paired t-test).

Acute Ethanol Intoxication Impairs the Translocation of Conventional PKC

The activation of receptor-coupled PLC and subsequent spikes in $[\text{Ca}^{2+}]_i$ are expected to drive the translocation of conventional isoforms of PKC from the cytosol to the membrane where the kinase binds and is further activated by DAG. In the next series of experiments, we investigated the actions of ethanol on the translocation of conventional PKC β II to the membrane. Hepatocyte cultures were transduced overnight with adenoviruses encoding enhanced green fluorescent protein (EGFP) tagged PKC β II (gift from R. Rizzuto). Live-cell confocal imaging was used to measure the distribution of GFP fluorescence in hepatocytes expressing PKC β II-EGFP before (Figure 6A, left) and after stimulating with 1 μM ATP (Figure 6A, right). Image analysis revealed that purinergic stimulation induced a decrease in GFP fluorescence in the perinuclear region and accumulation of the probe in a plasma membrane domain. We next measured hormone-induced $[\text{Ca}^{2+}]_i$ responses and PKC β II translocation simultaneously in fura-2-loaded and PKC β II-EGFP expressing hepatocytes. A ratio was calculated between the reciprocal changes GFP fluorescence intensity in membrane versus the

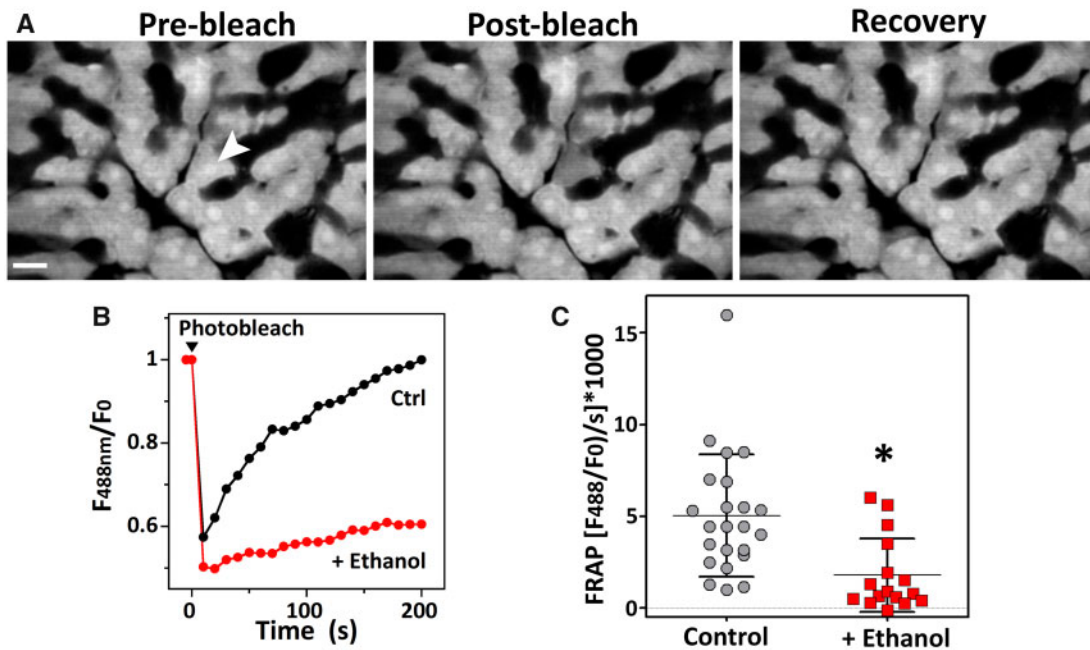


Figure 4. Acute Ethanol Perfusion Suppresses Gap Junction Communication. (A) Confocal images (211 $\mu\text{m} \times 141 \mu\text{m}$) of a calcein/AM loaded perfused rat liver. Images show the laser-induced photobleaching and recovery of the cell highlighted by the arrowhead. White scale bar denotes 20 μm . (B and C) Fluorescence recovery after photobleaching (FRAP) assays were carried out before and after perfusion with 20 mM ethanol. (B) Traces are the normalized fluorescence intensity changes from two different cells within the same hepatic lobule. (C) Summary data showing the initial rates of fluorescence recovery in the absence or presence of 20 mM ethanol. Data points are recovery rates from individual cells. Mean \pm SD are also shown, $n = 3$ livers, *Paired t-test $P < 0.05$.

cytoplasm to evaluate the translocation of PKC. The traces in Figure 6B show the measurements of vasopressin-induced oscillations in $[\text{Ca}^{2+}]_i$ and parallel translocation of PKC β II-EGFP to and from the membrane. The insert on the right depicts Ca^{2+} and PKC responses on an expanded time scale and normalized to baseline values for clarity. The data show that onset of the $[\text{Ca}^{2+}]_i$ spike occurs prior to detectable changes in PKC β II-EGFP distribution, whereas the PKC β II-EGFP is still translocating to the membrane after the $[\text{Ca}^{2+}]_i$ spike has peaked (Figure 6B). PKC β II-EGFP translocated back to the cytosol during the declining phase of the Ca^{2+} spike, but clearly lagged behind the Ca^{2+} signal (Figure 6B).

The addition of ethanol suppressed the magnitude and frequency of vasopressin-induced Ca^{2+} oscillations, and these effects translated into decreases in the extent and frequency of PKC β II-EGFP translocation to the membrane (Figure 6C). The actions of ethanol on hormone-induced PKC β II translocation were similar in both fura-2/AM-loaded and unloaded hepatocytes (Figure 6D). We calculated the peak vasopressin-induced increases in the fura-2 ratio and extent of PKC translocation, as well as the rates of rise, rates of fall, and AUC for both parameters, before and after ethanol treatment in the same cell. Summary results are shown in Figure 6E and F and Table 2. The acute ethanol intoxication significantly decreased the magnitude of both hormone-induced $[\text{Ca}^{2+}]_i$ spikes and translocation of PKC to membrane (Figure 6E and F). Moreover, ethanol slowed down the kinetics of the Ca^{2+} spikes and the translocation of PKC (Table 2).

The Actions of Ethanol on Hormone-Induced Ca^{2+} Signaling Require Ethanol Metabolism

The main pathway for ethanol clearance in hepatocytes is the sequential oxidation by alcohol dehydrogenase (ADH) to produce acetaldehyde followed by the conversion of acetaldehyde

into acetate in the mitochondrial matrix by aldehyde dehydrogenase (ALDH).⁶⁴ The catabolism of ethanol causes a marked reduction of NAD^+ to NADH , leading to a rise in the NADH/NAD^+ redox ratio. This stimulates the production of reactive oxygen species (ROS),^{65,66} which can potentiate the opening of IP_3 receptors.^{67,68} Hepatocyte cultures were incubated for 30 min in the presence of 4-methylpyrazole, an alcohol dehydrogenase inhibitor, or cyanamide, an aldehyde dehydrogenase inhibitor, prior to the addition of submaximal concentrations of phenylephrine. Cyanamide is a prodrug that requires bioconversion into the active compound necessitating the preincubation step.⁶⁹

The frequency of phenylephrine-induced Ca^{2+} oscillations was reduced in a dose-dependent manner with increasing concentrations of ethanol in primary cultured hepatocytes (Figure 7B, red symbols). Pretreating hepatocytes with 4-methylpyrazole to block ADH prevented the ethanol-induced increase in NADH fluorescence, consistent with the inhibition of ethanol metabolism (Figure 7C). This inhibition of the key first step of ethanol metabolism in liver largely ablated the effects of low ethanol concentrations on hormone-induced Ca^{2+} oscillations (Figure 7A). The dose-response for ethanol inhibition of Ca^{2+} oscillations in the presence of 4-methylpyrazole (Figure 7B, green symbols) shows a substantial right-shift compared to ethanol alone. At higher concentrations of ethanol (≥ 30 mM) there was a residual effect to reduce the frequency of agonist-induced Ca^{2+} oscillations, which may reflect a direct effect of ethanol or the possibility that saturating concentrations of ethanol can partially overcome the competitive block of 4-methylpyrazole. The finding that the acute effects of ethanol on hormone-stimulated Ca^{2+} signaling depend, at least in part, on ethanol metabolism via ADH is an important finding that can point to potential mechanisms.

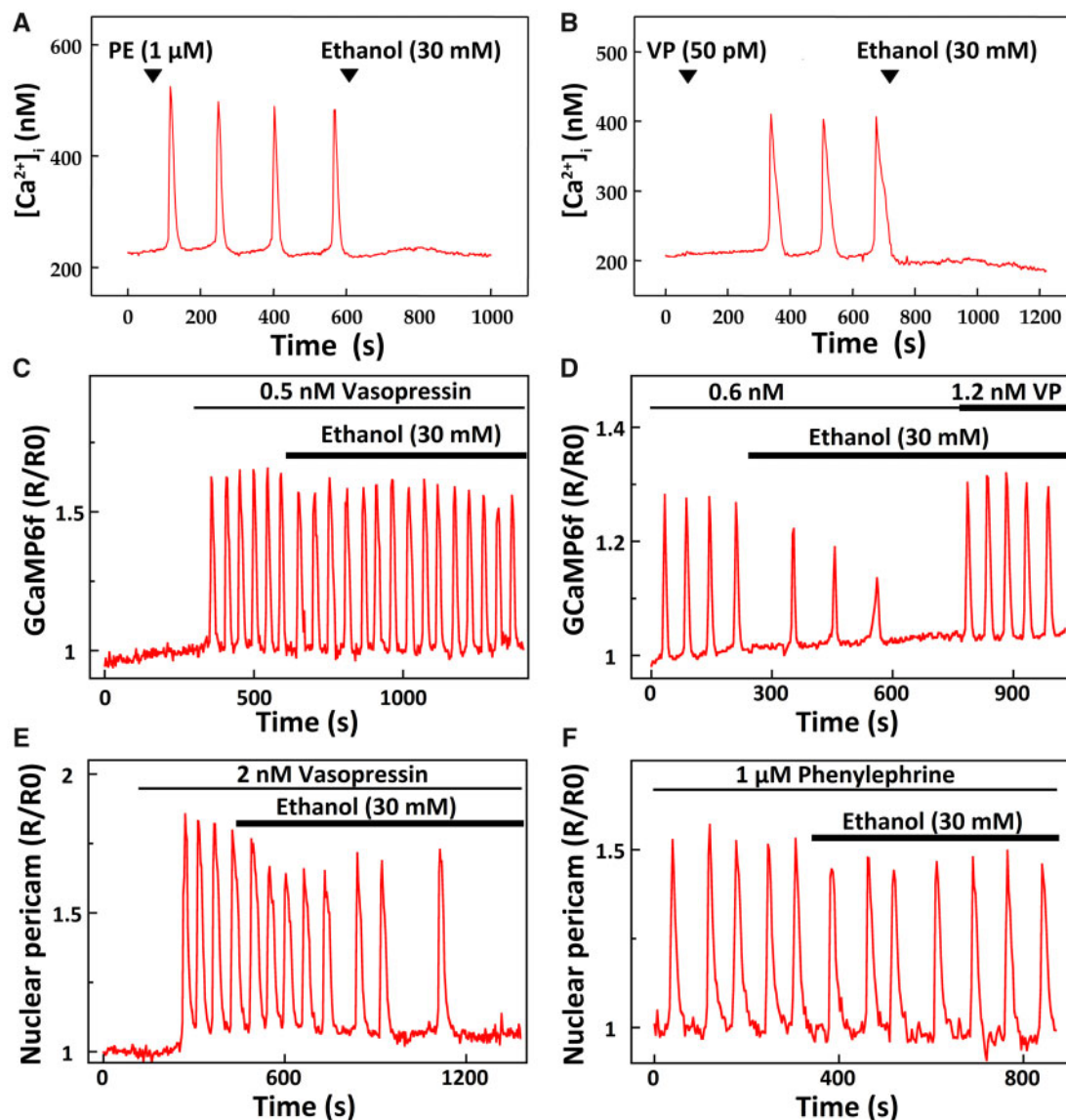


Figure 5. Acute Ethanol Treatment Suppresses Hormone-Induced Ca^{2+} Oscillations in Isolated Hepatocytes. (A and B) Freshly-plated rat hepatocytes were loaded with fura-2/AM then stimulated with submaximal concentrations of phenylephrine (PE) or vasopressin (VP) where indicated by the arrowheads. After 5–10 min, the cultures were acutely treated with 30 mM ethanol. In separate studies, hepatocytes were transfected with GCaMP6f (C and D) or ratiometric-pericam-nu (E and F) and then maintained in primary culture overnight. Traces are single-cell Ca^{2+} responses illustrating the effects of ethanol treatment on the magnitude of agonist-induced cytosolic (C and D) or nuclear (E and F) Ca^{2+} spikes.

We further investigated the role of ethanol metabolism by inhibiting the clearance of the ethanol metabolite acetaldehyde with cyanamide. In contrast to the inhibition of ADH with 4-methylpyrazole, ALDH inhibition potentiated the effects of ethanol on agonist-induced Ca^{2+} oscillations (Figure 7B blue symbols). The IC_{50} values for ethanol-induced inhibition of Ca^{2+} oscillations were 5 mM, 79 mM or 0.8 mM in the presence of ethanol alone, 4-methylpyrazole plus ethanol or cyanamide plus ethanol, respectively. In a separate set of experiments, hepatocyte cultures were pretreated with the antioxidants *N,N'*-dimethylthiourea (1 mM, DMTU) or *N,N'*-diphenyl 1,4-phenylenediamine (5 μM , DPPD). DMTU has been shown previously to suppress ROS production and apoptosis in hepatocytes during acute ethanol intoxication,^{70,71} while the addition of DPPD inhibits oxidant-induced increases in lipid peroxidation.^{72,73}

The data show that neither DMTU nor DPPD pretreatment blocked the inhibitory effects of ethanol on agonist-induced Ca^{2+} oscillations (Figure 7D and E). Moreover, treatment with Trolox (100 μM), a water-soluble vitamin E analog, or DMSO (100 mM) at concentrations that scavenge hydroxyl radicals⁷⁴ were also ineffective at blocking the effects of ethanol on Ca^{2+} signaling. The fold-change in the frequency of phenylephrine-induced Ca^{2+} oscillations was 0.51 ± 0.2 in the presence of ethanol alone, while in cells treated with DMTU, DPPD, Trolox, or DMSO prior to the addition of ethanol, the fold-change was 0.38 ± 0.1 , 0.37 ± 0.2 , 0.43 ± 0.1 , or 0.56 ± 0.1 respectively (mean \pm SD, $n = 2\text{--}4$ separate hepatocyte preparations). These data indicate that ethanol catabolism is required to suppress IP_3 -dependent Ca^{2+} signals and implicate acetaldehyde, but not the formation of ROS, as the underlying effector.

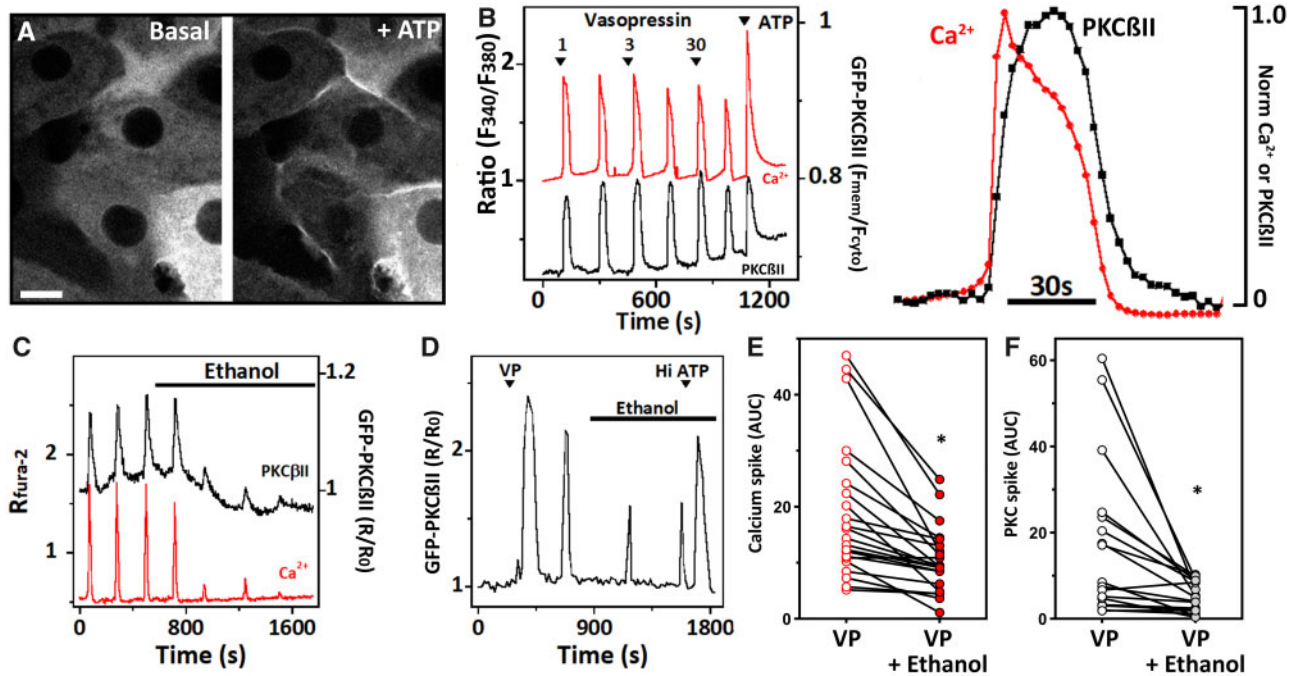


Figure 6. Effect of Ethanol on Hormone-Induced Translocation of PKC β II. Hepatocyte primary cultures were transduced overnight with adenoviruses encoding EGFP-tagged PKC β II then used in confocal microscopy (A and D) or coloaded with fura-2/AM and used in wide-field fluorescence studies (B and C). (A) Representative confocal images showing translocation of PKC β II-EGFP induced by 1 μ M ATP. White scale bar denotes 15 μ m. (B) Simultaneous measurement of vasopressin-induced Ca $^{2+}$ oscillations and PKC β II-EGFP translocation. Translocation of PKC β II was monitored by taking the ratio of the GFP fluorescence intensity changes in the membrane versus cytosol. Insert a single Ca $^{2+}$ spike and translocation of PKC β II on an expanded time scale and normalized to the initial ratio and peak increase for clarity. (C) Effect of 30 mM ethanol on vasopressin-induced Ca $^{2+}$ oscillations and translocation of PKC β II or (D) the translocation of PKC β alone. The PKC β II membrane:cytosol ratio was normalized to the initial ratio. In Panel C, Ca $^{2+}$ increases were induced by the addition of 1 nM vasopressin. (E and F) Summary data showing the AUC for hormone-induced [Ca $^{2+}$] $_i$ spikes and the normalized PKC β translocation ratio in the presence of vasopressin (VP) and after the acute addition of 30 mM ethanol (VP + ethanol). Data were calculated from 2 to 4 baseline-separated [Ca $^{2+}$] $_i$ spikes or translocation of PKC β II before and after the addition of 30 mM ethanol. *Significantly different from hormone alone; $P < 0.01$, paired t-test. $n = 17$ –22 cells from three independent hepatocyte preparations.

Table 1. Effect of Acute Ethanol Treatment on the Frequency of Vasopressin-Induced Ca $^{2+}$ Oscillations in the ex vivo Perfused Rat Liver

Ethanol (mM)	Periportal	Pericentral	<i>n</i>
0.3	0.97	0.88	1
1	0.83 \pm 0.07	0.78 \pm 0.06	5
10	0.57 \pm 0.03	0.52 \pm .03	3
20	0.54 \pm 0.06	0.51 \pm 0.03	8
50	0.47	0.41	2
300	0.50	0.44	1

The frequency of Ca $^{2+}$ spiking was calculated before and after addition of the indicated concentrations of ethanol and expressed as a fold-change. Data are the means \pm SD or the means if less than three livers were used in the experiment, n = number of liver preparations.

Ethanol Does Not Perturb IP $_3$ Receptor Function, but Inhibits the Hormone-Stimulated Formation of IP $_3$

To assess the effects of acute ethanol treatment on IP $_3$ receptor function, cultured hepatocytes were coloaded with fluo-4/AM and caged-IP $_3$, and then exposed to a series of UV flashes to photorelease IP $_3$. Photolysis of caged IP $_3$ produces a variety of [Ca $^{2+}$] $_i$ increases in hepatocytes ranging from no response, through to single Ca $^{2+}$ spikes, repetitive Ca $^{2+}$ oscillations, to maximal peak and plateau types of Ca $^{2+}$ signals.^{29,75} Importantly, we have previously shown that the Ca $^{2+}$ spikes produced by uncaging IP $_3$ are predominately mediated by the

Table 2. Effect of Ethanol Treatment on Vasopressin-Induced Calcium Increases and PKC Translocation

	Vasopressin	Vasopressin + 30 mM ethanol
Δ Ratio (Ca $^{2+}$)	0.89 \pm 0.5	0.59 \pm 0.3*
Ratio rise/s	0.13 \pm 0.01	0.08 \pm 0.06*
Ratio fall/s	-0.05 \pm 0.03	-0.04 \pm 0.02*
Ratio AUC	19.1 \pm 12.4	10.4 \pm 5.8*
Δ PKC	0.5 \pm 0.4	0.23 \pm 0.2*
PKC rise/s	0.04 \pm 0.03	0.03 \pm 0.04 ^{ns}
PKC fall/s	-0.02 \pm 0.02	-0.01 \pm 0.01*
PKC AUC	17.7 \pm 18.3	5.2 \pm 3.4*

Primary cultured hepatocytes expressing PKC β II-EGFP were loaded with fura-2/AM and then stimulated with vasopressin to evoke baseline-separated [Ca $^{2+}$] $_i$ oscillations. Ethanol (30 mM) was added 10–20 min after hormone stimulation. The data are the means \pm SD for the peak increase in the fura-2 excitation ratio or PKC translocation, the rates of rise and fall in fura-2 ratio or PKC translocation, and the AUC for fura-2 ratio or PKC translocation. Data were calculated from 2 to 4 spikes before and after addition of ethanol in the same cell, $n = 22$ cells from three separate cell preparations.

*Statistically different from vasopressin alone, paired t-test, $P < 0.05$. ns, not significant.

intrinsic properties of the IP $_3$ receptors with little to no contribution from receptor-coupled PLC activity.^{75,76} The addition of 30 mM ethanol did not qualitatively alter the types of Ca $^{2+}$ responses induced by uncaging IP $_3$ compared to control (Figure 8A), nor did

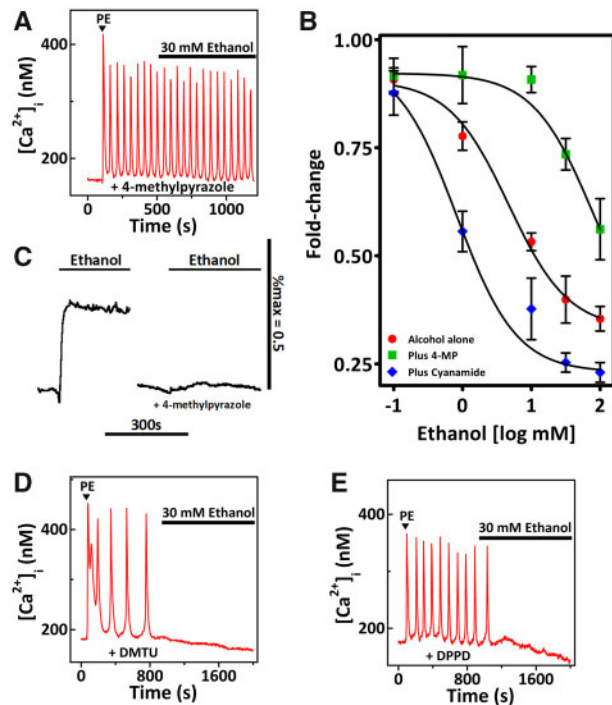


Figure 7. Ethanol Metabolism Is Required for the Inhibitory Actions of Ethanol on Ca^{2+} Oscillations. (A–C) Hepatocytes were pretreated for 30 min with 500 μM 4-methylpyrazole (4-MP), 100 μM cyanamide, or buffer prior to data acquisition. (A) Representative single-cell Ca^{2+} trace showing the lack of effect of ethanol on Ca^{2+} spiking in the presence of 4-MP. (B) Summary data showing the effects of increasing concentrations of ethanol (0.1–100 mM) on the frequency of phenylephrine (PE)-induced Ca^{2+} oscillations. The changes in frequency are expressed as a fold-change for each cell analyzed. Data points are the means \pm SEM, $n = 3$ –12 separate experiments carried out in 20 different hepatocytes preparations with 25–75 cells per measurement. (C) The increases in hepatic NAD(P)H fluorescence in response to ethanol (100 mM) were determined in the absence (left) or presence (right) of 4-MP. NAD(P)H fluorescence was normalized to the initial intensity and to the maximal fluorescence intensities recorded after the addition of rotenone plus β -hydroxybutyrate; $n = 50$ –100 cells/assay. (D and E) Hepatocytes incubated with N,N' -dimethylthiourea (1 mM, DMTU) or N,N' -diphenyl 1,4-phenylenediamine (5 μM , DPPD) for 60–90 min prior to data acquisition. Traces are single-cell Ca^{2+} responses depicting the effects of ethanol on Ca^{2+} spiking in the presence of the indicated antioxidants.

ethanol treatment affect the amplitude or width of IP_3 -dependent Ca^{2+} spikes (Figure 8B and C). Moreover, the addition of 100 μM acetaldehyde to digitonin-permeabilized hepatocyte suspensions did not affect Ca^{2+} -uptake into internal stores (not shown) or the amount of Ca^{2+} mobilized by IP_3 . The addition of 500 nM IP_3 released 2.3 ± 0.2 nmoles Ca^{2+} /mg protein compared to 3.3 ± 1.0 nmoles Ca^{2+} /mg protein in the absence and presence of acetaldehyde, respectively (mean \pm SD, $n = 3$ hepatocyte preparations, ns). These data suggest that these pharmacologically relevant concentrations of ethanol or its metabolite, acetaldehyde, do not alter the properties of IP_3 receptors.

We initially utilized biochemical assays to investigate the actions of ethanol on hormone-stimulated PLC activity in cultured hepatocytes. These assays were unable to detect any differences between vasopressin-stimulated increases in IP_3 mass or in the accumulation of $[\text{H}^3]$ -inositol phosphates in the absence or presence of 30 mM ethanol, which may reflect the relatively low sensitivity of these assays at physiological hormone concentrations that give rise to Ca^{2+} oscillations. As an alternative approach, hepatocytes were transfected overnight with a recombinant IP_3 -sensitive biosensor IRIS-1⁵⁶ and then

loaded with the Ca^{2+} indicator dye Indol-1/AM. We have previously used this protocol to demonstrate that there are cross-coupled oscillations of IP_3 and Ca^{2+} during hormone stimulation of hepatocytes, and that these reflect a requirement for positive feedback of Ca^{2+} on PLC activity to generate the hormone-induced Ca^{2+} oscillations.⁷⁷ As reported previously,⁷⁷ the onset of each Ca^{2+} and IP_3 spike lags slightly behind the concomitant Ca^{2+} spike (Figure 8D). In order to increase the signal to noise of the IRIS-1 FRET ratio, IP_3 spike traces were averaged from 2 to 4 sequential oscillations aligned to the rising phase of the individual spikes. This allowed quantitation of the IP_3 spike kinetics following hormone stimulation before (Figure 8E, left) and after (Figure 8E, right) the addition of 30 mM ethanol. Ethanol treatment decreased the amplitude of the vasopressin-stimulated IP_3 oscillations, slowed the rates of rise and fall of the individual IP_3 spikes and decreased the AUC (Figure 8F and G; Table 3). Taken together, our findings suggest that ethanol inhibits receptor-coupled PLC activity which, in turn, suppresses the cross-coupling between IP_3 and Ca^{2+} dynamics that initiates and drives the rapid rising phase of the oscillatory Ca^{2+} spikes.

Discussion

The natural progression of alcohol-related liver disease (ALD) follows a well-characterized pattern.⁷⁸ Ethanol consumption initially induces steatosis or fatty liver over the course of a few days to several weeks of heavy drinking and this phenotype can manifest in virtually all alcohol drinkers.⁷⁹ Alcohol-induced fatty liver can progress onto liver inflammation and fibrosis in a subset of alcoholics, but this usually requires decades of excessive alcohol consumption.⁷⁸ Despite the overt toxicity of ethanol and its metabolite, acetaldehyde, the factors driving the progression from the early stages of alcoholic fatty liver, which are reversible, to more advanced stages of liver injury remain debatable and areas of active research.^{78,80–83} Ethanol is a relatively nonspecific drug with pleiotropic effects on most organs in the body and, thus ethanol consumption can initiate multiple mechanisms, in both the liver and extrahepatic tissues, that can potentially contribute to the development of liver injury.^{78,81} These mechanisms include ethanol-dependent changes in the gut microbiome and disruption of gut barrier function,⁸² adaptive responses in hepatic ethanol metabolism,⁸³ hyperactivation of lipolysis in adipose tissue,⁸⁴ acute pancreatitis,⁸⁵ stimulation of the innate immune system,⁸⁶ and alterations in the composition and secretion of exosomes.⁸⁷ These changes can combine with environmental factors such as the consumption of dietary unsaturated fats⁸⁸ to produce a multifaceted and complex pathology. We have proposed that enhanced receptor-coupled PI-PLC activity induced by long-term and repeated exposure to ethanol may be another mechanism contributing to hepatic injury^{17,29}; the inappropriate activation of PLC-linked signaling cascades could underlie some of the pleiotropic actions of ethanol on liver function.

In this study, we investigated both the acute effects of ethanol on $[\text{Ca}^{2+}]_i$ and its actions on hormone-induced Ca^{2+} signaling. Our studies using an ex vivo perfused liver model indicate that concentrations of ethanol up to and above the legal intoxication limit (20–30 mM) do not have a direct effect on $[\text{Ca}^{2+}]_i$. Ethanol in the perfusate had to be increased to 100 mM or more before inducing Ca^{2+} spikes in a small percentage of cells in the intact liver. The biological significance of these ethanol-induced Ca^{2+} responses is not readily clear. Blood alcohol concentrations

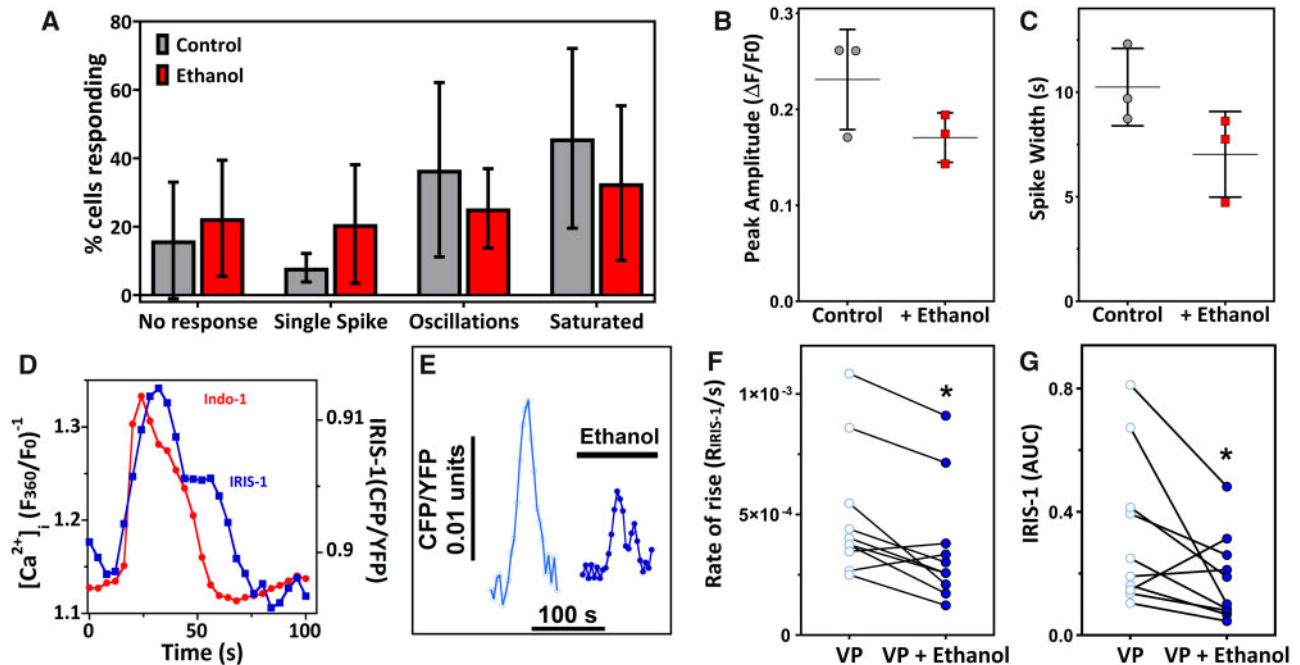


Figure 8. Ethanol Treatment Does Not Affect IP₃ Receptor Sensitivity but Suppresses Hormone-Induced Production of IP₃. Rat hepatocytes were coloaded with cell-permeant caged-IP₃ and fluo-4/AM (A–C). IP₃ was uncaged with 4 UV pulses from a nitrogen-charged UV laser in the absence or presence of 30 mM ethanol (5 min pretreatment). (A) Summary data showing the categories of Ca²⁺ responses observed after uncaging IP₃. The effects of ethanol treatment on the amplitude (B) and width (C) of Ca²⁺ spikes induced by uncaging IP₃. Data points are the means of 2–3 replicate determinations carried out for each hepatocyte preparation (*n* = 3). (D–G) Hepatocytes transfected overnight with IRIS-1 were loaded with Indo-1/AM and then stimulated with vasopressin (1–3 nM). (D) Representative traces showing the simultaneously measurement of vasopressin-induced increases in [Ca²⁺]_i (red trace) and IRIS-1 emission ratio (blue trace) (E) Vasopressin-induced increases in the IRIS-1 emission ratio were aligned to the rising phase of the spike. Traces are the averaged responses calculated from three IRIS-1 spikes before and after the addition of ethanol (30 mM). (F and G) Summary data showing the rates of rise and AUC for vasopressin-induced spikes in the IRIS-1 emission ratio before (VP) and after the addition of 30 mM ethanol (VP + ethanol). Data were calculated from 2 to 4 IRIS-1 spikes before and after addition of ethanol in the same cell. *Significantly different from vasopressin alone; *P* < 0.01, paired *t*-test. *n* = 10 cells from two different hepatocyte preparations and three independent transfections.

Table 3. Effect of Ethanol Treatment on Vasopressin-Induced Increases in IRIS-1 Emission Ratio

	Vasopressin	Vasopressin + 30 mM Ethanol
ΔIRIS-1	8.5e-3 ± 4.7e-3	5.9e-3 ± 4e-3*
Rise/s	5.0e-4 ± 3e-4	3.7e-4 ± 3e-4*
Fall/s	-3.3e-4 ± 2e-4	-2.7e-4 ± 2e-4 ^{ns}
AUC	0.33 ± 0.24	0.18 ± 0.14*

Hepatocytes expressing IRIS-1 were loaded with Indo-1/AM and then stimulated with vasopressin (VP, 1–3 nM) to evoke baseline separated Ca²⁺ oscillations. Ethanol (30 mM) was added 10–20 min after vasopressin stimulation. The data are the means ± SD for the peak VP-induced increases the IRIS-1 emission ratio, the rates of rise and fall of the IRIS-1 increase, and the AUC for the IRIS-1 spike. Data were calculated from 2 to 4 IRIS-1 spikes before and after addition of ethanol in the same cell, *n* = 10 cells from two different cell preparations and three independent transfections. *Statistically different from vasopressin alone, paired *t*-test, *P* < 0.05. ns, not significant.

in excess of 100 mM are not observed in healthy volunteers given ethanol,^{23,89} however, there are reports of alcoholics presenting at emergency departments with plasma ethanol concentrations between 100 and 170 mM,^{22,23} as well as a single report of an alcoholic who survived a blood alcohol level of 300 mM.⁹⁰ Thus, although high concentrations of ethanol can directly activate the G-protein-coupled PLC to generate IP₃ and elicit Ca²⁺ signals in the liver,^{17,18,20,91} this probably only occurs after bouts of excessive binge drinking in chronic alcoholics. In this context, we have previously demonstrated that chronic

ethanol consumption enhances the efficacy of hormones to stimulate Ca²⁺ signaling by sensitizing receptor-coupled PLC activity in liver,²⁹ which may be a compensatory mechanism for the acute inhibitory effects of ethanol described here. If such a compensatory mechanism also increases the efficacy of ethanol to mobilize internal Ca²⁺ stores, then an acute binge on top of chronic ethanol consumption could produce a prolonged and sustained rise in [Ca²⁺]_i that could cause liver injury. It is currently unknown if chronic ethanol consumption or feeding can modify the Ca²⁺ responses induced by acute ethanol treatment.

Bearing in mind the range of blood alcohol levels normally encountered, the more relevant effects of ethanol described here are to suppress hormonal signaling. Acute ethanol intoxication has been reported to affect multiple targets that could contribute to the inhibition of phosphoinositide-dependent Ca²⁺ signals in rat hepatocytes.^{25,28} However, these previous experiments were carried out predominately with high concentrations of ethanol (>100 mM), raising questions of whether these targets are also affected at pharmacologically achievable concentrations of ethanol. Our data show that low doses of ethanol potentially suppress hormone-induced Ca²⁺ oscillations and the parallel translocation of conventional PKCβ to the membrane. The half-maximal inhibitory concentration of ethanol on Ca²⁺ oscillations was in the low millimolar range, which is similar to the reported *K*_ms of the two main enzymes that metabolize ethanol to acetaldehyde in liver: ADH (*K*_m ≈ 2 mM)⁹² and CYP2E1 (*K*_m ≈ 10 mM).⁶⁴ By using 4-methylpyrazole, which is a potent inhibitor of both ADH and CYP2E1, we showed that the inhibitory effects of ethanol on agonist-induced Ca²⁺

oscillations are largely dependent on ethanol metabolism. The effects of 10 mM ethanol and below were completely blocked by 4-methylpyrazole, and this compound also significantly reduced the inhibitory effects of ethanol up to 100 mM (Figure 7B). The residual inhibitory effect of high ethanol concentrations could reflect a direct action of ethanol on IP₃-dependent Ca²⁺ signaling, or it could be because 4-methylpyrazole does not completely block ethanol oxidation by CYP2E1.⁹³

Another important effect of ethanol observed in our ex vivo perfused rat liver studies was the marked reduction in cell-to-cell communication in the presence of ethanol. This clearly underlies the suppression of hepatocyte-to-hepatocyte propagation of Ca²⁺ signals in the intact perfused liver, and hence to the disruption of the organization and coordination of intercellular Ca²⁺ waves during agonist perfusion in the presence of ethanol. Moreover, the reduction in cell-cell communication will reduce integrated lobular signaling, which we recently reported plays a key role in generating the global response of the liver to glycogenic hormones.⁴⁷ We have shown previously that the coordination of lobular Ca²⁺ waves during hormonal stimulation of the liver is dependent on coupling of cell signaling through gap junctions,¹⁰ and this study shows that acute ethanol interferes with this coupling. This is consistent with previous work showing the inhibitory effects of ethanol on gap junctions, and significantly, this effect was also reported to require ethanol metabolism.⁶¹

Taken together, the findings discussed above indicate that the inhibitory actions of pharmacologically relevant doses of ethanol on hepatic Ca²⁺ signaling are mediated by metabolically derived acetaldehyde, and are most likely not a direct effect of ethanol. It should be noted that ethanol also reacts with long-chain fatty acids to produce fatty acid ethyl esters (FAEEs) through a nonoxidative pathway catalyzed by fatty acid ethyl ester synthase.⁹⁴ The nonoxidative production of FAEEs is thought to be the primary mechanism whereby ethanol induces alcoholic pancreatitis.^{16,85} These studies indicate that pancreatic acinar cell injury is caused by a sustained rise in [Ca²⁺]_i triggered by FAEE dependent Ca²⁺ release from the ER and store-operated Ca²⁺ entry.^{16,95,96} The role of FAEEs in alcoholic liver disease is less clear. The activity of fatty acid ethyl ester synthase in rat tissues is ≈60-fold higher in the pancreas compared to liver.⁹⁷ Moreover, in human hepatoma cell lines, nonoxidative production of FAEEs accounts for <1% of total ethanol metabolism, and the detection of cellular FAEEs above baseline values requires high concentrations of ethanol (80 mM) and long incubation periods (hours).^{98,99} These studies suggest that FAEEs may not be involved in, at least, the acute effects of ethanol on Ca²⁺ signaling in hepatocytes. Nevertheless, it is possible that this mechanism could play a role in liver damage in chronic alcoholics. Our studies show acetaldehyde is responsible for impairing Ca²⁺ signaling, but do not address how acetaldehyde can affect receptor-coupled PLC activity. Acetaldehyde can form both stable and unstable adducts with hepatic proteins, particularly on lysine residues,^{100,101} and such acetaldehyde-adducts could modify or impair the function of the receptor-stimulated Ca²⁺ signaling machinery.

We also considered ethanol-induced increases in cellular NADH or the production of ROS as potential mediators of ethanol action on Ca²⁺ signaling. Several lines of evidence that argue against a role for NADH: 1) ethanol-induced increases in NADH are maximal at ≈2 mM in the perfused liver (not shown, but see Kashiwagi et al.¹⁰²), whereas the effects of ethanol on agonist-induced Ca²⁺ oscillations are not (Figures 3B and 7B); 2) an increase in cytosolic NADH levels does not appear to affect

the activity of PLC¹⁰³; and 3) inhibiting ALDH enhances the effects of ethanol on Ca²⁺ oscillations while decreasing NADH formation (Figure 7B). Acute ethanol intoxication has been reported to induce the formation of ROS in mitochondria.⁶⁶ However, the effects of ethanol on agonist-induced Ca²⁺ signaling were not prevented by the ROS scavengers DPPD and DMTU. Notably, production of mitochondrial ROS and cell death induced by the reoxygenation of anoxic hepatocytes has been shown to be markedly suppressed by DPPD.¹⁰⁴ Our data show that similar concentrations of DPPD cannot block or reverse the actions of ethanol on agonist-induced Ca²⁺ oscillations (Figure 7E). These data indicate that ethanol metabolism to increase NADH and stimulate ROS formation does not play a significant role in the short-term effects of ethanol on agonist-induced Ca²⁺ oscillations.

In conclusion, our data show that pharmacologically relevant concentrations of ethanol suppress receptor-stimulated PLC activity and slow down the associated oscillatory increases in both [IP₃] and [Ca²⁺]_i. We have previously demonstrated that rapid dynamic changes in IP₃ levels are required to produce the repetitive, large-amplitude Ca²⁺ oscillations induced by PLC-linked hormones.⁷⁷ By decreasing the rate of rise and the peak increase in [IP₃], ethanol partially uncouples the positive feedback between IP₃ and Ca²⁺ during the rising phase of the Ca²⁺ spike, leading to early termination of the [Ca²⁺]_i increase or complete cessation of Ca²⁺ spiking. This idea is consistent with the observation that increasing the concentration of hormone, and presumably also the rates of IP₃ production, reverses the effects of ethanol on the frequency of Ca²⁺ oscillations and amplitude of the Ca²⁺ spike (Figures 3 and 5). In the short term, the acute inhibitory effects of ethanol on receptor-coupled PLC will perturb the normal hormonal regulation of hepatic metabolism. However, after long-term ethanol exposure, the liver overcomes the acute inhibitory actions of ethanol on IP₃ production by increasing the efficacy of hormones to stimulate PLC activity.²⁹ This adaptive response would enable hepatocytes to respond to Ca²⁺-mobilizing hormones and increase metabolic output even in the presence of high levels of circulating ethanol. However, when blood alcohol levels fall during times of sobriety this compensatory mechanism could lead to the overstimulation of receptor-coupled PLC and hyperactivation of downstream Ca²⁺ and PKC-sensitive targets.

Acknowledgments

We thank Dr. K. Mikoshiba (RIKEN) for the pIRIS-1 construct, Dr. A. Miyawaki (RIKEN) for pRatiometric-pericam-nu construct, Dr. D. Kim (HHMI) for pGP-CMV-GCaMP6f, and Dr. R. Rizzuto (University of Padua) for the PKCβII-EGFP adenovirus particles (Ad-PKCβII-EGFP). We thank Kerri Anne Stellato, Shwetal Metha, and Mimi Shon for technical assistance in carrying out the hepatocyte imaging studies and Dr. Sandip Patel for helpful discussions. Graphical abstract was created with BioRender.com.

Authors' Contributions

L.D.G. performed the intact perfused liver and single hepatocyte imaging studies. P.J.B. carried out the flash photolysis of caged IP₃ experiments and analysis. L.D.G., A.P.T., and J.B.H. designed the study. L.D.G. wrote the manuscript. P.J.B., A.P.T., and J.B.H. reviewed and edited the article.

Funding

This work was supported by National Institutes of Health Grants AA017752 (L.D.G.), AA018873 (J.B.H.), DK082954 and AI099277 (A.P.T.) and The Thomas P. Infusino Endowment (A.P.T.).

Conflict of Interest Statement

The authors state that they have no conflicts of interest related to this study.

References

- Berridge MJ. Inositol trisphosphate and calcium signalling. *Nature* 1993;361(6410):315–325.
- Thomas AP, Bird GS, Hajnoczky G, Robb-Gaspers LD, Putney JW Jr. Spatial and temporal aspects of cellular calcium signaling. *FASEB J* 1996;10(13):1505–1517. <http://www.ncbi.nlm.nih.gov/pubmed/8940296>. Published 1996/11/01.
- Glancy B, Balaban RS. Role of mitochondrial Ca^{2+} in the regulation of cellular energetics. *Biochemistry* 2012;51(14):2959–2973.
- Amaya MJ, Nathanson MH. Calcium signaling in the liver. *Compr Physiol* 2013;3(1):515–539.
- Bartlett PJ, Gaspers LD, Pierobon N, Thomas AP. Calcium-dependent regulation of glucose homeostasis in the liver. *Cell Calcium* 2014;55(6):306–316.
- Patel S, Joseph SK, Thomas AP. Molecular properties of inositol 1,4,5-trisphosphate receptors. *Cell Calcium* 1999;25(3):247–264.
- Putney JW. Pharmacology of store-operated calcium channels. *Mol Interv* 2010;10(4):209–218.
- Rooney TA, Sass EJ, Thomas AP. Characterization of cytosolic calcium oscillations induced by phenylephrine and vasopressin in single fura-2-loaded hepatocytes. *J Biol Chem* 1989;264(29):17131–17141.
- Rooney TA, Sass EJ, Thomas AP. Agonist-induced cytosolic calcium oscillations originate from a specific locus in single hepatocytes. *J Biol Chem* 1990;265(18):10792–10796.
- Gaspers LD, Thomas AP. Calcium signaling in liver. *Cell Calcium* 2005;38(3–4):329–342.
- Hajnoczky G, Robb-Gaspers LD, Seitz MB, Thomas AP. Decoding of cytosolic calcium oscillations in the mitochondria. *Cell* 1995;82(3):415–424.
- Robb-Gaspers LD, Burnett P, Rutter GA, Denton RM, Rizzuto R, Thomas AP. Integrating cytosolic calcium signals into mitochondrial metabolic responses. *Embo J* 1998;17(17):4987–5000.
- Lin C, Hajnoczky G, Thomas AP. Propagation of cytosolic calcium waves into the nuclei of hepatocytes. *Cell Calcium* 1994;16(4):247–258.
- Garcin I, Tordjmann T. Calcium signalling and liver regeneration. *Int J Hepatol* 2012;2012:630670.
- Oliva-Vilarnau N, Hankeova S, Vorrink SU, Mkrtchian S, Andersson ER, Lauschke VM. Calcium signaling in liver injury and regeneration. *Front Med (Lausanne)* 2018;5:192.
- Petersen OH, Tepikin AV, Gerasimenko JV, Gerasimenko OV, Sutton R, Criddle DN. Fatty acids, alcohol and fatty acid ethyl esters: toxic Ca^{2+} signal generation and pancreatitis. *Cell Calcium* 2009;45(6):634–642.
- Hoek JB, Thomas AP, Rooney TA, Higashi K, Rubin E. Ethanol and signal transduction in the liver. *FASEB J* 1992;6(7):2386–2396.
- Hoek JB, Thomas AP, Rubin R, Rubin E. Ethanol-induced mobilization of calcium by activation of phosphoinositide-specific phospholipase C in intact hepatocytes. *J Biol Chem* 1987;262(2):682–691.
- Saso K, Nomura T, Higashi K, Hoek JB. Differentiation between ethanol-induced phospholipase C activation and ethanol-dependent desensitization of hormonal response in rat hepatocytes (abstr). *Hepatology* 1993;18:275A.
- Reinlib L, Akinshola E, Potter JJ, Mezey E. Ethanol-induced increases in $[\text{Ca}^{2+}]_i$ and inositol (1,4,5) triphosphate in rat hepatocytes. *Biochem Biophys Res Commun* 1990;173(3):774–780.
- Zhang BH, Farrell GC. Ethanol perturbs receptor-operated cytosolic free calcium concentration signals in cultured rat hepatocytes. *Gastroenterology* 1997;113(2):641–648.
- Lindblad B, Olsson R. Unusually high levels of blood alcohol? *JAMA* 1976;236(14):1600–1602.
- Adachi J, Mizoi Y, Fukunaga T, Ogawa Y, Ueno Y, Imamichi H. Degrees of alcohol intoxication in 117 hospitalized cases. *J Stud Alcohol* 1991;52(5):448–453.
- Bertola A, Mathews S, Ki SH, Wang H, Gao B. Mouse model of chronic and binge ethanol feeding (the NIAAA model). *Nat Protoc* 2013;8(3):627–637.
- Higashi K, Hoek JB. Ethanol causes desensitization of receptor-mediated phospholipase C activation in isolated hepatocytes. *J Biol Chem* 1991;266(4):2178–2190.
- Hoek JB, Nomura T, Higashi K. Ethanol and phospholipid dependent signal transduction: The view from the liver. In: CGS Alling, ed. *Alcohol, Cell Membranes, and Signal Transduction in Brain*. New York, NY: Plenum Press, 1993: 219–233.
- Hoek JB, Thomas AP. *Ethanol and Intracellular Signaling: from Molecules to Behavior*. Bethesda, MD: U.S. Department of Health and Human Services, Public Health Service, National Institute of Health, National Institute on Alcohol Abuse and Alcoholism, 2000.
- Renard-Rooney DC, Seitz MB, Thomas AP. Inhibition of hepatic inositol 1,4,5-trisphosphate receptor function by ethanol and other short chain alcohols. *Cell Calcium* 1997;21(5):387–398.
- Bartlett PJ, Antony AN, Agarwal A, et al. Chronic alcohol feeding potentiates hormone-induced calcium signalling in hepatocytes. *J Physiol* 2017;595(10):3143–3164.
- Fu S, Yang L, Li P, et al. Aberrant lipid metabolism disrupts calcium homeostasis causing liver endoplasmic reticulum stress in obesity. *Nature* 2011;473(7348):528–531.
- Park SW, Zhou Y, Lee J, Lee J, Ozcan U. Sarco(endo)plasmic reticulum Ca^{2+} -ATPase 2b is a major regulator of endoplasmic reticulum stress and glucose homeostasis in obesity. *Proc Natl Acad Sci USA* 2010;107(45):19320–19325.
- Period CN, Gustavo Oliveira A, Guerra MT, et al. Hepatic inositol 1,4,5 trisphosphate receptor type 1 mediates fatty liver. *Hepatol Commun* 2017;1(1):23–35.
- Wilson CH, Ali ES, Scrimgeour N, et al. Steatosis inhibits liver cell store-operated Ca^{2+} entry and reduces ER Ca^{2+} through a protein kinase C-dependent mechanism. *Biochem J* 2015;466(2):379–390.
- Wang Y, Li G, Goode J, et al. Inositol-1,4,5-trisphosphate receptor regulates hepatic gluconeogenesis in fasting and diabetes. *Nature* 2012;485(7396):128–132.
- Khamphaya T, Chukijrungrat N, Saengsirisuwan V, et al. Nonalcoholic fatty liver disease impairs expression of the type II inositol 1,4,5-trisphosphate receptor. *Hepatology* 2018; 67(2):560–574.

36. Ozcan L, Cristina de Souza J, Harari AA, Backs J, Olson EN, Tabas I. Activation of calcium/calmodulin-dependent protein kinase II in obesity mediates suppression of hepatic insulin signaling. *Cell Metab* 2013;18(6):803–815.
37. Ozcan L, Wong CC, Li G, et al. Calcium signaling through CaMKII regulates hepatic glucose production in fasting and obesity. *Cell Metab* 2012;15(5):739–751.
38. Shibao K, Hirata K, Robert ME, Nathanson MH. Loss of inositol 1,4,5-trisphosphate receptors from bile duct epithelia is a common event in cholestasis. *Gastroenterology* 2003;125(4):1175–1187.
39. Kruglov EA, Gautam S, Guerra MT, Nathanson MH. Type 2 inositol 1,4,5-trisphosphate receptor modulates bile salt export pump activity in rat hepatocytes. *Hepatology* 2011;54(5):1790–1799.
40. Lagoudakis L, Garcin I, Julien B, et al. Cytosolic calcium regulates liver regeneration in the rat. *Hepatology* 2010;52(2):602–611.
41. Ali ES, Rychkov GY, Barritt GJ. Deranged hepatocyte intracellular Ca(2+) homeostasis and the progression of non-alcoholic fatty liver disease to hepatocellular carcinoma. *Cell Calcium* 2019;82:102057.
42. Prevarskaya N, Skryma R, Shuba Y. Calcium in tumour metastasis: new roles for known actors. *Nat Rev Cancer* 2011;11(8):609–618.
43. Cui C, Merritt R, Fu L, Pan Z. Targeting calcium signaling in cancer therapy. *Acta Pharm Sin B* 2017;7(1):3–17.
44. Rodrigues MA, Gomes DA, Leite MF, et al. Nucleoplasmic calcium is required for cell proliferation. *J Biol Chem* 2007;282(23):17061–17068.
45. Mangla A, Guerra MT, Nathanson MH. Type 3 inositol 1,4,5-trisphosphate receptor: a calcium channel for all seasons. *Cell Calcium* 2020;85:102132.
46. Roberts-Thomson SJ, Chalmers SB, Monteith GR. The calcium-signaling toolkit in cancer: remodeling and targeting. *Cold Spring Harb Perspect Biol* 2019;11(8). doi: 10.1101/cshperspect.a035204.
47. Gaspers LD, Pierobon N, Thomas AP. Intercellular calcium waves integrate hormonal control of glucose output in the intact liver. *J Physiol* 2019;597(11):2867–2885.
48. Robb-Gaspers LD, Thomas AP. Coordination of Ca2+ signaling by intercellular propagation of Ca2+ waves in the intact liver. *J Biol Chem* 1995;270(14):8102–8107.
49. Gaspers LD, Patel S, Morgan AJ, Anderson PA, Thomas AP. Monitoring generation and propagation of calcium signals in multicellular preparations. In: A Tepikin, ed. *Calcium Signalling: A Practical Approach*. Oxford: Oxford University Press, 2001:155–175.
50. Robb-Gaspers LD, Anderson PA, Thomas AP. Imaging whole organs. In: R Rizzuto, C Fasolato, eds. *Imaging Living Cells*. New York, NY: Springer Inc., 1998:115–139.
51. Monck JR, Oberhauser AF, Keating TJ, Fernandez JM. Thin-section ratiometric Ca2+ images obtained by optical sectioning of fura-2 loaded mast cells. *J Cell Biol* 1992;116(3):745–759.
52. Thevenaz P, Ruttimann UE, Unser M. A pyramid approach to subpixel registration based on intensity. *IEEE Trans Image Process* 1998;7(1):27–41.
53. Gaspers LD, Thomas AP. Calcium-dependent activation of mitochondrial metabolism in mammalian cells. *Methods* 2008;46(3):224–232.
54. Smaili SS, Stellato KA, Burnett P, Thomas AP, Gaspers LD. Cyclosporin A inhibits inositol 1,4,5-trisphosphate-dependent Ca2+ signals by enhancing Ca2+ uptake into the endoplasmic reticulum and mitochondria. *J Biol Chem* 2001;276(26):23329–23340.
55. Morgan AJ, Thomas AP. Single cell and subcellular measurement of intracellular Ca2+ concentration ([Ca2+]i). *Methods Mol Biol* 1999;114:93–123.
56. Matsu-ura T, Michikawa T, Inoue T, Miyawaki A, Yoshida M, Mikoshiba K. Cytosolic inositol 1,4,5-trisphosphate dynamics during intracellular calcium oscillations in living cells. *J Cell Biol* 2006;173(5):755–765.
57. Thomas AP, Hoek JB, Rubin E. Elevation of inositol 1,4,5-trisphosphate levels after acute ethanol treatment of rat hepatocytes. *Ann N Y Acad Sci* 1987;492(1):250–255.
58. Hoek JB, Higashi K. Effects of alcohol on polyphosphoinositide-mediated intracellular signaling. *Ann N Y Acad Sci* 1991;625:375–387. doi: 10.1111/j.1749-6632.1991.tb33865.x.
59. Ghosh Dastidar S, Warner JB, Warner DR, McClain CJ, Kirpich IA. Rodent models of alcoholic liver disease: role of binge ethanol administration. *Biomolecules* 2018;8(1). doi: 10.3390/biom8010003.
60. Thomas AP, Robb-Gaspers LD, Rooney TA, Hajnóczky G, Renard-Rooney DC, Lin C. Spatial organization of oscillating calcium signals in liver. *Biochem Soc Trans* 1995;23(3):642–648.
61. Abou Hashieh I, Mathieu S, Besson F, Gerolami A. Inhibition of gap junction intercellular communications of cultured rat hepatocytes by ethanol: role of ethanol metabolism. *J Hepatol* 1996;24(3):360–367.
62. Clair C, Chalumeau C, Tordjmann T, et al. Investigation of the roles of Ca(2+) and InsP(3) diffusion in the coordination of Ca(2+) signals between connected hepatocytes. *J Cell Sci* 2001;114(Pt 11):1999–2007.
63. Nathanson MH, Rios-Velez L, Burgstahler AD, Mennone A. Communication via gap junctions modulates bile secretion in the isolated perfused rat liver. *Gastroenterology* 1999;116(5):1176–1183.
64. Zakhari S. Overview: how is alcohol metabolized by the body? *Alcohol Res Health* 2006;29(4):245–254.
65. Bailey SM, Cunningham CC. Acute and chronic ethanol increases reactive oxygen species generation and decreases viability in fresh, isolated rat hepatocytes. *Hepatology* 1998;28(5):1318–1326.
66. Bailey SM, Pietsch EC, Cunningham CC. Ethanol stimulates the production of reactive oxygen species at mitochondrial complexes I and III. *Free Radic Biol Med* 1999;27(7–8):891–900.
67. Joseph SK, Young MP, Alzayady K, et al. Redox regulation of type-I inositol trisphosphate receptors in intact mammalian cells. *J Biol Chem* 2018;293(45):17464–17476.
68. Kaplin AI, Snyder SH, Linden DJ. Reduced nicotinamide adenine dinucleotide-selective stimulation of inositol 1,4,5-trisphosphate receptors mediates hypoxic mobilization of calcium. *J Neurosci* 1996;16(6):2002–2011.
69. Koppaka V, Thompson DC, Chen Y, et al. Aldehyde dehydrogenase inhibitors: a comprehensive review of the pharmacology, mechanism of action, substrate specificity, and clinical application. *Pharmacol Rev* 2012;64(3):520–539.
70. Kurose I, Higuchi H, Miura S, et al. Oxidative stress-mediated apoptosis of hepatocytes exposed to acute ethanol intoxication. *Hepatology* 1997;25(2):368–378.
71. Higuchi H, Adachi M, Miura S, Gores GJ, Ishii H. The mitochondrial permeability transition contributes to acute ethanol-induced apoptosis in rat hepatocytes. *Hepatology* 2001;34(2):320–328.
72. Rubin R, Farber JL. Mechanisms of the killing of cultured hepatocytes by hydrogen peroxide. *Arch Biochem Biophys* 1984;228(2):450–459.

73. Masuda Y, Yamamori Y. Histological detection of lipid peroxidation following infusion of tert-butyl hydroperoxide and ADP-iron complex in perfused rat livers. *Jpn J Pharmacol* 1991;56(2):133–142.
74. Cederbaum AI, Rubin E. The oxidation of acetaldehyde by isolated mitochondria from various organs of the rat and hepatocellular carcinoma. *Arch Biochem Biophys* 1977;179(1):46–66.
75. Bartlett PJ, Metzger W, Gaspers LD, Thomas AP. Differential regulation of multiple steps in inositol 1,4,5-trisphosphate signaling by protein kinase C shapes hormone-stimulated Ca²⁺ oscillations. *J Biol Chem* 2015;290(30):18519–18533.
76. Bartlett PJ, Cloete I, Sneyd J, Thomas AP. IP₃-dependent Ca(2+) oscillations switch into a dual oscillator mechanism in the presence of PLC-linked hormones. *iScience* 2020;23(5):101062.
77. Gaspers LD, Bartlett PJ, Politi A, et al. Hormone-induced calcium oscillations depend on cross-coupling with inositol 1,4,5-trisphosphate oscillations. *Cell Rep* 2014;9(4):1209–1218.
78. Seitz HK, Bataller R, Cortez-Pinto H, et al. Alcoholic liver disease. *Nat Rev Dis Primers* 2018;4(1):16.
79. Rubin E, Lieber CS. Alcohol-induced hepatic injury in nonalcoholic volunteers. *N Engl J Med* 1968;278(16):869–876.
80. Hoek JB, Cahill A, Pastorino JG. Alcohol and mitochondria: a dysfunctional relationship. *Gastroenterology* 2002;122(7):2049–2063.
81. Tsukamoto H, Machida K, Dynnyk A, Mkrtychyan H. "Second hit" models of alcoholic liver disease. *Semin Liver Dis* 2009;29(2):178–187.
82. Szabo G. Gut-liver axis in alcoholic liver disease. *Gastroenterology* 2015;148(1):30–36.
83. Zhong Z, Lemasters JJ. A unifying hypothesis linking hepatic adaptations for ethanol metabolism to the proinflammatory and profibrotic events of alcoholic liver disease. *Alcohol Clin Exp Res* 2018;42(11):2072–2089.
84. Wang ZG, Dou XB, Zhou ZX, Song ZY. Adipose tissue-liver axis in alcoholic liver disease. *World J Gastrointest Pathophysiol* 2016;7(1):17–26.
85. Clemens DL, Wells MA, Schneider KJ, Singh S. Molecular mechanisms of alcohol associated pancreatitis. *World J Gastrointest Pathophysiol* 2014;5(3):147–157.
86. Nagy LE. The role of innate immunity in alcoholic liver disease. *Alcohol Res* 2015;37(2):237–250.
87. Eguchi A, Lazaro RG, Wang J, et al. Extracellular vesicles released by hepatocytes from gastric infusion model of alcoholic liver disease contain a MicroRNA barcode that can be detected in blood. *Hepatology* 2017;65(2):475–490.
88. Kirpich IA, Miller ME, Cave MC, Joshi-Barve S, McClain CJ. Alcoholic liver disease: update on the role of dietary fat. *Biomolecules* 2016;6(1):1.
89. Laitinen K, Lamberg-Allardt C, Tunnenen R, et al. Transient hypoparathyroidism during acute alcohol intoxication. *N Engl J Med* 1991;324(11):721–727.
90. Johnson RA, Noll EC, Rodney WM. Survival after a serum ethanol concentration of 1 1/2%. *Lancet* 1982;2(8312):1394.
91. Rooney TA, Hager R, Rubin E, Thomas AP. Short chain alcohols activate guanine nucleotide-dependent phosphoinositidase C in turkey erythrocyte membranes. *J Biol Chem* 1989;264(12):6817–6822.
92. Julia P, Farres J, Pares X. Characterization of three isoenzymes of rat alcohol dehydrogenase. Tissue distribution and physical and enzymatic properties. *Eur J Biochem* 1987;162(1):179–189.
93. Feierman DE, Cederbaum AI. Inhibition of microsomal oxidation of ethanol by pyrazole and 4-methylpyrazole in vitro. Increased effectiveness after induction by pyrazole and 4-methylpyrazole. *Biochem J* 1986;239(3):671–677.
94. Ricardo JD-O. Oxidative and non-oxidative metabolomics of ethanol. *Current Drug Metabolism* 2016;17(4):327–335.
95. Criddle DN, Raraty MGT, Neoptolemos JP, Tepikin AV, Petersen OH, Sutton R. Ethanol toxicity in pancreatic acinar cells: mediation by nonoxidative fatty acid metabolites. *Proc Natl Acad Sci USA* 2004;101(29):10738–10743.
96. Huang W, Booth DM, Cane MC, et al. Fatty acid ethyl ester synthase inhibition ameliorates ethanol-induced Ca²⁺-dependent mitochondrial dysfunction and acute pancreatitis. *Gut* 2014;63(8):1313.
97. Hamamoto T, Yamada S, Hirayama C. Nonoxidative metabolism of ethanol in the pancreas; implication in alcoholic pancreatic damage. *Biochem Pharmacol* 1990;39(2):241–245.
98. Dan L, Cluette-Brown JE, Kabakibi A, Laposata M. Quantitation of the mass of fatty acid ethyl esters synthesized by Hep G2 cells incubated with ethanol. *Alcohol Clin Exp Res* 1998;22(5):1125–1131.
99. Laposata EA, Harrison EH, Hedberg EB. Synthesis and degradation of fatty acid ethyl esters by cultured hepatoma cells exposed to ethanol. *J Biol Chem* 1990;265(17):9688–9693.
100. Medina VA, Donohue TM Jr, Sorrell MF, Tuma DJ. Covalent binding of acetaldehyde to hepatic proteins during ethanol oxidation. *J Lab Clin Med* 1985;105(1):5–10.
101. Tuma DJ, Casey CA. Dangerous byproducts of alcohol breakdown—focus on adducts. *Alcohol Res Health* 2003;27(4):285–290.
102. Kashiwagi T, Ji S, Lemasters JJ, Thurman RG. Rates of alcohol dehydrogenase-dependent ethanol metabolism in periportal and pericentral regions of the perfused rat liver. *Mol Pharmacol* 1982;21(2):438–443.
103. Liu M, Shi G, Yang KC, et al. Role of protein kinase C in metabolic regulation of the cardiac Na(+) channel. *Heart Rhythm* 2017;14(3):440–447.
104. Kim JS, Wang JH, Lemasters JJ. Mitochondrial permeability transition in rat hepatocytes after anoxia/reoxygenation: role of Ca²⁺-dependent mitochondrial formation of reactive oxygen species. *Am J Physiol Gastrointest Liver Physiol* 2012;302(7):G723–G731.